Université du Québec à Trois Rivières

Thesis presented at Université du Québec à Trois Rivières
in partial fulfillment for the degree of
Master of Science in Biophysics

by

Darren C. Goetze

Characterization of a Photoelectrochemical Cell Utilizing Photosynthetic Membranes and An Application to the Study of Electron Transport

December 1990

"...our knowledge of biotic phenomena contains a vast range of unspecifiable elements, and biology remains, in consequence, a descriptive science heavily relying on trained perception. It is immeasurably rich in things we know and cannot tell. Such is life and such is our knowledge of life; on such grounds are based the triumphs of biology."

-Michael Polanyi

"i'm bound by the beauty
i'm bound by desire
i'm bound to keep returning
i'm bound by the beauty of light
the slightest change
the constant rearrange
of light..."

- Jane Siberry

ABSTRACT

Thylakoid membranes isolated from spinach have generated photocurrents in a photoelectrochemical cell. The activation effect of methyl viologen, a PS I electron acceptor known to increase the magnitude of the photocurrent generated, has been characterized. The effects of three enzymes on the photocurrent have been studied. The enzymes were superoxide dismutase, glucose oxidase and catalase. All three are shown to inhibit the photocurrent to specific enzyme-dependent degrees. These results are used to demonstate that electrons are transfered to the working electrode via an oxygen mediated pathway similar to a Mehler type reaction. Further, the activity originates from PS I with oxygen as the acceptor and PS II as the donor. Evidence is also given to show the direct relationship between the concentration of chlorophyll and the photocurrent produced and catalase is demonstrated to be a non-competitive inhibitor of the photoreduction. Cyclic voltammograms of PS I- and PS II enriched membranes reveal the role of each in photocurrent generation and that the two can be separated if provided the appropriate acceptor/donor. Action spectra obtained for all three types of membranes show sample-specific variations in their contributions to the photocurrent.

Having established the photoelectrochemical cell as a new approach to monitoring pseudocyclic electron transport, a study using isolated and commercially obtained ferredoxin

suggests that the site of *in vivo* oxygen reduction is ferredoxin:$NADP^+$ oxioreductase. This result is discussed in terms of its metabolic consequence.

RESUME

Dans une cellule photoélectrochimique il est possible de générer un photocourant en présence de membranes thylacoïdiennes isolées de feuilles d'épinard. Ce photocourant est de nature photosynthétique puisque le DCMU, un inhibiteur bien connu du transport d'électrons au niveau du PS II, inhibe toute photoactivité. De plus, l'oxygène est impliqué dans la production de ce photocourant tel que démontré par sa présence dans les balayages de voltamétrie cyclique et par le fait qu'un barbottage a l'azote provoque une perte du photocourant.

Les données obtenues à partir des potentiels médians de la courbe d'oxydation en fonction du logarythme naturel de la vitesse de ces balayages indiquent qu'une réaction chimique précède les phénomènes électrochimiques au niveau de l'électrode. L'inhibition présentée en présence de catalase démontre que cette réaction est de type Mehler et, par le fait même, que les électrons sont transférés à l'électrode de travail par l'intermédiaire d'un transport impliquant l'oxygène suivant un mécanisme similaire au transport pseudocyclique in vivo. Il a été aussi possible de démontrer que la catalase est un inhibiteur non-compétif de la génération du photocourant. L'expérimentation a également établi que ce transport subit une inhibition enzymatique spécifique en présence de la superoxide dismutase et de la glucose oxydase.

La production du photocourant est stimulée par le méthyl viologène, un accepteur d'électrons au niveau du PS I. Ce phénomène implique la réaction de Mehler. L'augmentation produite par cet accepteur est également sensible à la catalase. De plus, la corrélation entre les données obtenues avec le méthyl viologen grâce à la cellule photoélectrochimique et celles observées à l'aide d'une électrode de type Clark (consommation d'oxygène), démontre que la cellule photoélectrochimique procure une mesure quantitative de la réduction de l'oxygène par les membranes thylacoïdiennes. On peut également observer une relation directe entre la concentration de chlorophylle utilisée et le photocourant produit.

En absence d'un accepteur d'électrons, tel que le DCBQ, les membranes enrichies en PS II se révèlent incapables de produire un photocourant. Il en est de même pour les extraits enrichis en PS I auxquels l'ajout d'un donneur artificiel d'électrons, la duroquinone, permet la génération d'un fort photocourant. Cependant, le voltamogramme cyclique des fractions membranaires de PS I démontrent que le donneur utilisé, même s'il a la possibilité de donner deux électrons, ne semble donner que celui à faible potentiel, afin de produire un photocourant sensible aux effets du méthyl viologène et de la catalase.

Dans les trois préparations étudiées (thylacoïdes, PS I et PS II), il a été démontré que le gain d'électrons par les accepteurs constitue l'étape limitante. Les spectres

d'action de ces trois préparations, dévoilent par ailleurs que les pigments contribuent de façon spécifique à la génèse du photocourant.

Les résultats obtenus avec la cellule photoélectrochimique prouvent sans équivoque qu'elle constitue une approche nouvelle des plus prometteuses pour mesurer le transport d'électrons pseudocyclique. Cette méthode nous a amené à entreprendre l'étude fondamentale de ce transport d'électrons. Ainsi, deux préparations distinctes de ferrédoxine dont l'une, pure, isolée au laboratoire, et l'autre commerciale, contenant la ferrédoxine et la ferrédoxine:$NADP^+$ réductase, ont montré deux résultats divergents. Ces résultats suggèrent que le site de réduction de l'oxygène est situé sur la ferrédoxine:$NADP^+$ réductase. Il nous permettent de proposer un modèle impliquant les conséquences métaboliques au niveau des plantes possédant un transport d'électrons pseudocyclique.

ACKNOWLEDGEMENTS

I would like to firstly thank my project supervisor, Dr. Robert Carpentier, for his guidance, flexibility and financial support in bringing this work to fruition.

In addition, I'd like to thank Dr. Doug Bruce, my B. Sc. thesis supervisor, for his contribution of both maniacal threats, motivating me to seriously investigate studying at Trois Rivières in the first place, and his now much appreciated efforts helping me to get accepted to the program. Actually, he just wanted to be rid of me.

I would like to thank Dr. Angela Agostiano for her unique way of teaching me the secrets of electrochemistry: long hours of work, characterized by exhaustion and baggy eyes, followed by her ambrosial cuisine (always unassumingly and modestly prepared) was certainly the way to indelibly impress the lessons onto my brain (cell). Warm and with a zest for life, she was immediately and always my friend.

Two people in particular have made especially appreciated technical contributions and are deserving of my perpetual gratitude (or, better, 1.44 $) : Emmanual Nenonéné, (mon grand frère, taught me the world was not just for whites - I always suspected) for his help with cellulose chromatography and Monique Bareil, for her help with SDS-PAGE - not to mention her warm and cheery disposition (and she SMELLED so good).

I'd also like to expressedly thank the people who have made my experience in Québec more fun than practical jokes

at a proctology clinic: ShowerMan ("Truly the cleanest person I ever met", said MazolaMan), his Wife (who has been known to exaggerate JUST a little), Josée (someone of wonderful understated elegance and unfathomable tender kindness - was oviously destined to be an electrochemist), Serge (for cider stories and other Tales Of The Québecois), Mimi (La - ahem - toucheuse), Nathalie B. (once acurately described to me as un p'tit soleil), Je'F (aka Mr. Soundeffects), Johanne (Mom), Chantal (how can someone so small be so organized?), Stephane (the Shark), Sylvain (Monsieur Coiffe), Andrianne (oo-la-la) and The Others (blahblahblah, hohoho and you know who you are, etc.)

These have been particularly poignant and difficult, yet exciting and dynamic, times to be in Québec, what with the latest altercations in the Canadian constitutional Hundred Years War (definately no pun intended) and the violent, careening emergence of native affairs onto the national psyche (however you define "national"). To those who care, I have been paying constant attention and I have learned much, much more than just science and a new language in the last two years.

In learning, I hope to have taught. By resisting outdated stereotypic labels. By challenging your accepted ideas. I immodestly hope to have made some small contribution to your understanding as well.

You **were** paying attention, weren't you?

TABLE OF CONTENTS

TABLE OF CONTENTS (cont'd)

LIST OF FIGURES

LIST OF FIGURES (cont'd)

LIST OF TABLES

LIST OF ABBREVIATIONS

Asc - L-ascorbate

ATP - adenosine 5'-triphosphate

Chl - chlorophyll

Cyt b_6f - cytochrome b_6f complex

DCBQ - 2,5-dichloro-p-benzoquinone

DCMU - 3-(3,4-dichlorophenyl)-1,1-dimethylurea

DHA - dehydroascorbate

DQ - tetramethyl-p-benzoquinone

ENDOR - electron nuclear double resonance spectroscopy

$E_{p/2}$ - half peak potential

ESR - electron spin resonance spectroscopy

FMN - flavin mononucleotide

FNR - ferredoxin-$NADP^+$ oxioreductase

GSH, GSSG - glutathione and its oxidized form

LHC - light harvesting complex

MDA - monodehydroascorbate

$NADP^+$/NADPH - nicotinamide - adenine dinucleotide phosphate, oxidized form/reduced form

OEC - oxygen evolving complex

P680 - photochemically active chlorophyll of PS II

P700 - photochemically active chlorophyll of PS I

Pheo - pheophytin

PS - photosystem

SCE - saturated calomel electrode

SHE - standard hydrogen electrode

SOD - superoxide dismutase

INTRODUCTION

I

Previous to this project, a single chambered electrochemical cell had been developed in this lab based on the design priorly presented by Allen and Crane (1976). The cell was shown to produce microampere currents in the presence of both light and photosynthetically competent samples. These samples included unfractionated thylakoid membranes (Lemieux and Carpentier, 1988a; Mimeault and Carpentier, 1989) and extracted PS II preparations (Lemieux and Carpentier, 1988b). Further, the photocurrents produced were able to be manipulated by exogenously added artificial electron acceptors that have been known to interact with photosynthetic systems. Unfortunately, the exact mechanism by which the photocurrent was propagated between biological samples and the electrodes of the photoelectrochemical cell was not well understood. Thus, this project undertook to elucidate that mechanism using a number of electrochemical techniques in conjunction with the photoelectrochemical cell. Firstly, potentiostatic electrochemistry was used to study the basic mechanism with the aid of exogenous amplifiers and inhibitors of the photocurrent and also the details of the effects of these agents. Secondly, cyclic voltammetry was used to examine the electroactive species involved in the photocurrent and their corresponding potentials. Lastly, the action spectra were measured to

determine the pigments that were involved with production of photocurrent.

II

The absorption of solar electromagnetic energy and its conversion to chemical energy occurs with impressive efficiency within the photosynthetic membranes of the multitudes of plant species inhabiting the Earth, including cyanobacteria, green algae and higher plants. In higher plants, the membranes are localized within the specialized organelles of epidermal and mesophyll cells, called chloroplasts. At this level, both structural and functional compartmentalization are found. The general interior of the chloroplast is called the stroma and it is here that the so-called "dark" reactions take place. The stroma's multitude of enzymes catalyze the essential reduction of carbon dioxide (carbon fixation) in utilizing the reducing power of NADPH and the energetic power of ATP. Also within the stroma is a membrane system, the thylakoids, folded into flattened disk-shaped, sac-like vesicles and organized into two domains: the appressed (granal) region and the non-appressed (stromal) region (Fig. 1, below). The vesicles are defined themselves by an internal compartment, the lumen, separated from the stroma by the thylakoid membrane. Dimensionally, they have a diameter of approximately 500 nm, a short axis of 20 nm and a thickness of 7 nm (Gräber, 1987). It is the thylakoid membranes that anchor the system of pigmented-

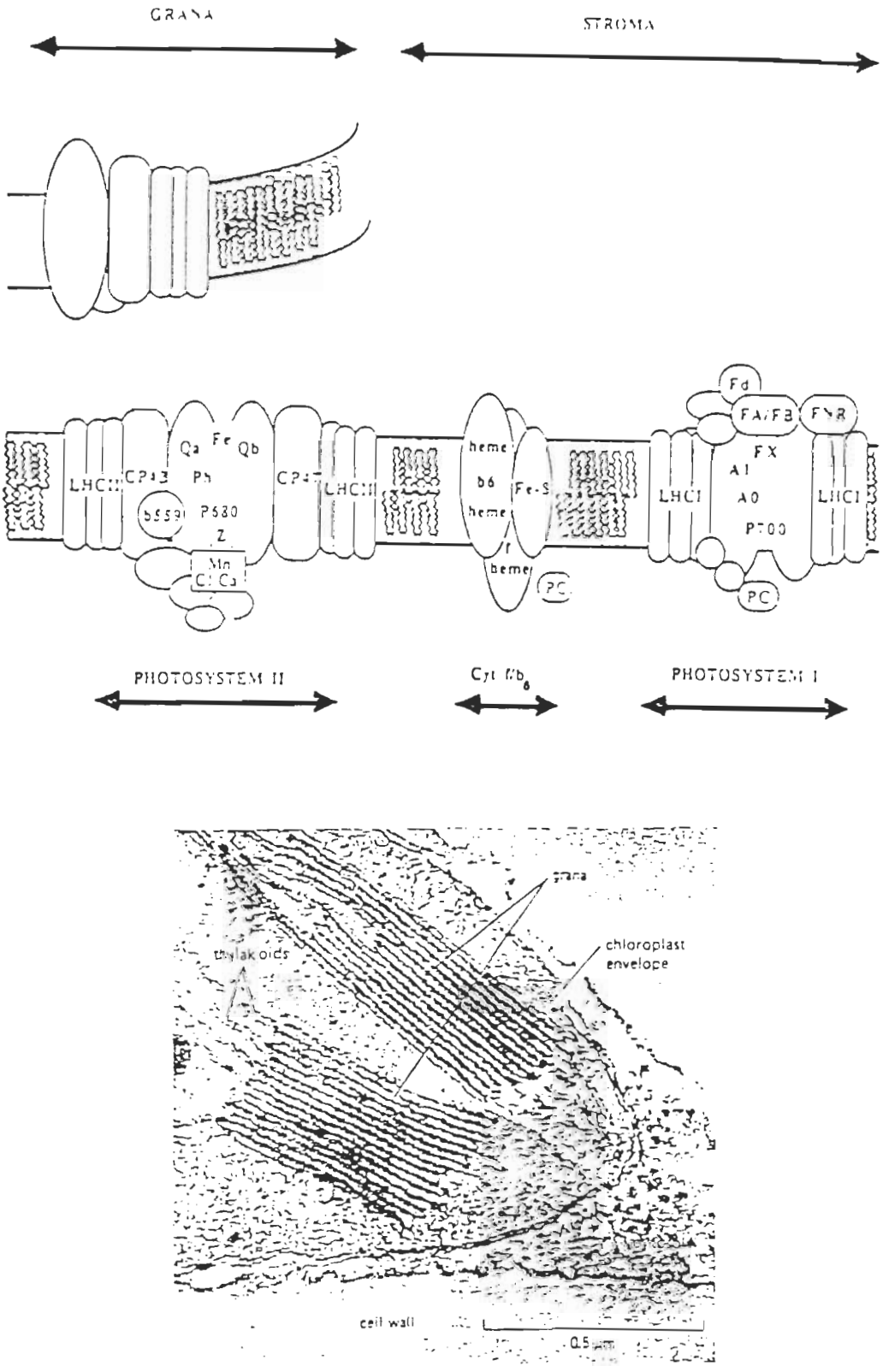

Figure 1. Top, arrangement of light reaction components within thylakoid membranes. Bottom, thylakoid domains within chloroplasts. (From Golbeck (1987) and Alberts et al (1983), respectively).

and heme-bearing polypeptides that carry out the "light" reactions, i.e. press advantage with specific frequencies of electromagnetic radiation to effect a series of oxidation/reduction reactions to ultimately produce the strong reductant NADPH and, indirectly, high energy ATP. The polypeptides are organized in a manner such that those active sites performing oxidation reactions are positioned within the membrane closer to the stromal phase and the sites performing reductive reactions, the lumen. A logical consequence of this heterogeneous redox orientation is the generation of a transmembrane electric field upon initiation of the redox events. Associated with the redox events are proteolytic reactions characterized by the active translocation of protons taken up in the stroma and released into the lumen, resulting in a pH gradient across the membrane. It is this electrochemical gradient that allows the passive return flow of protons back to the stroma, driving the formation of ATP, as proposed originally by the chemiosmotic mechanism (Mitchell, 1961).

More specifically, the polypeptides involved in the light reactions are arranged into a network of three components functioning cooperatively in series to transport electrons from water to $NADP^+$ during linear electron transport, according to the classic Z scheme (Hill and Bendall, 1960): photosystem I , cytochrome b_6f complex and photosystem II, as shown in Fig. 1, above. The photosystems are composed of a reaction center core, each containing

their respective sites of primary photochemistry P700 and P680, with its acceptor chain, and the associated antennae complexes (LHC I and LHC II, respectively) that contain both Chl-a and Chl-b (for an excellent review of chlorophylls, see Rüdiger and Schoch, 1988) and carotenoids. Spatially, the three are not distributed equally or homogeneously throughout the membrane but instead, the components exhibit the phenomena of lateral heterogeneity (Andersson and Anderson, 1980; Andersson and Haehnel, 1982; Anderson and Melis, 1983) whereby PS II is predominantly found in the appressed regions of thylakoids and PS I, in the non-appressed. The cyt b_6f is thought to be concentrated at the boundaries of the two regions (Cogdell, 1988). Of course, the components are not stationary within the membrane but have a lateral mobility as described by the fluid mosaic model (Singer and Nicolson, 1972).

Functionally, the initial processes occur in the antennae with the absorption of light quanta by the 200-250 Chl-a/b that make up the structure. The energy migrates towards the reaction center via a resonace transfer mechanism (Förster, 1948) and does so because P680 (or P700), being the longest wavelength pigment of the set, has the lowest energy in its excited state and thus, acts as an energy sink (Rutherford, 1988). This special molecule is itself capable of being directly excited by an appropriate photon but the effectiveness of the LHCs is in broadening the absorption cross section by more than two orders of

magnitude (Gräber, 1987). Once P680 or P700 become excited, the primary process of photosynthesis can occur. The energetics and kinetics of these processes are summarized in figure 2 (top and bottom, respectively).

The nature of P680 in higher plants has been controversially undecided in recent years (Rutherford, 1988; Nugent et al, 1989 and references therein) but very recent data seems to indicate P680 is a dimer of Chl-a (Barber, 1990). In any event, upon excitation of P680, there follows two electrogenically distinct steps (Trissl and Leibl, 1989): a charge separation occurs within 3 ps (Wasielewski et al, 1989), forming a radical pair consisting of oxidized $P680^+$ and a reduced pheo-a^- intermediate acceptor and a charge stabilization by forward electron transfer to the primary acceptor Q_A, a plastoquinone (Rutherford, 1988), with a time constant of 450 ps (Schatz et al, 1988). Concurrently, on the donor side of PS II, once the charge is stabilized, $P680^+$ will be reduced by Y (also referred to as Y_Z or Z) in a reaction characterized by multiphasic, ns kinetics (Andréasson and Vänngård, 1988). Y has been identified as a tyrosine residue (Barry and Babcock, 1987) whose oxidized state is a highly oxidizing neutral radical (Babcock et al, 1989). This radical is reduced by the oxygen evolving complex (OEC), a somewhat mysterious entity that utilizes as its low-energy electron source water, which is oxidized to molecular oxygen in the four electron process:

$$2\ H_2O \rightarrow\ O_2 + 4H^+ + 4e^-$$

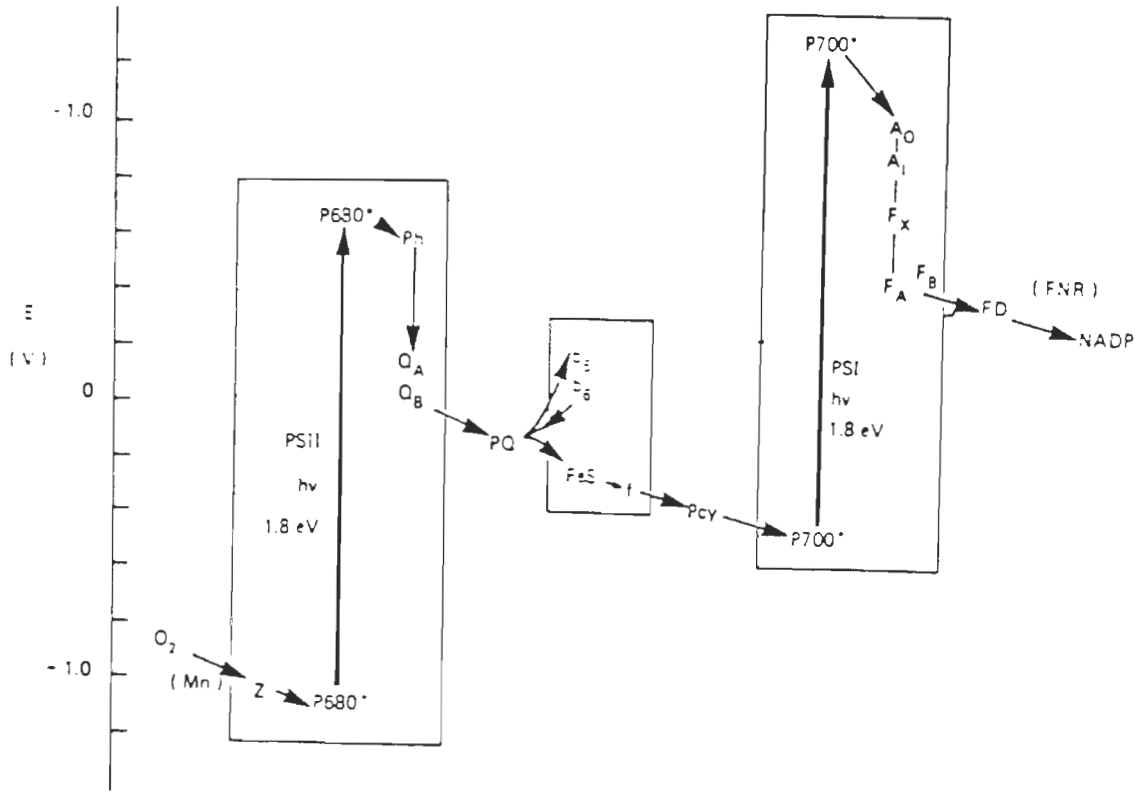

Redox potential

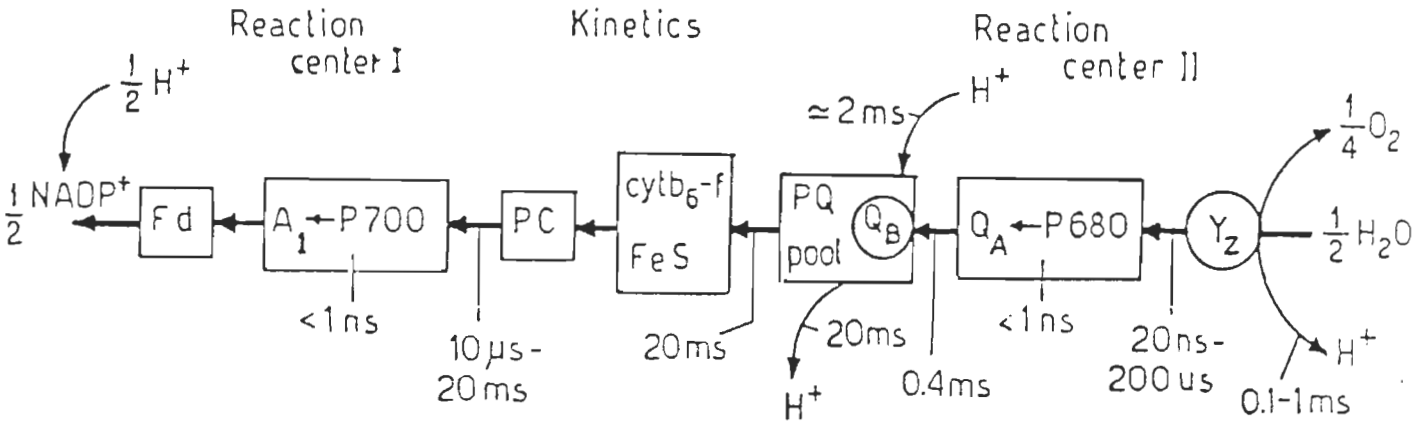

Figure 2. Energetics (top) and kinectics (bottom) of photosynthetic electron transport. Abbreviations as given in the text. (From Gregory (1989) and Gräber, (1987), respectively).

Given the stability of water, this is an extraordinary exploit implicating a formidable mechanism. It involves 4 manganese atoms controlably generating in a step-wise manner a reactive, unstable species capable of oxidizing water. The OEC is capable of five oxidation states designated S_0-S_4, with S_4 being the most oxidizing (for reviews of the OEC, see Bacock et al, 1989; Volkov, 1989). Also involved are a number of co-factors, including inorganic Ca^+ and Cl^-.

Returning to the acceptor side, in the subsequent electron transfer step, Q_A assumes the role of intermediary between one electron and two electron steps in PS II. Within 4 ms, Q_A fully reduces a subsequent plastoquinone, Q_B, to plastoquinol (Gräber,1987) in a reaction that involves the uptake of two protons from the stroma. Reduced and protonated, Q_B detaches from the reaction center complex (Crofts and Wraight, 1983; McPherson et al, 1990) and laterally diffuses within the membrane bilayer to the cyt b_6f complex (Rich and Bendall, 1980). The complex will reoxidize the plastoquinol and in doing so, releases its protons into the lumen (Malmström, 1989) and returns it as plastoquinone to the membrane moiety. These various redox forms of shuttling plastoquinone constitute the plastoquinone pool.

Functionally, the cyt b_6f complex is simply a four component redox system operating as a plastoquinone-plastocyanin oxioreductase but how this is mechanistically accomplished is not well understood (Joliot and Joliot,

1986; Adam and Malkin, 1987; Malmström, 1989). The redox components are two cyt b_6, a Rieske FeS center and a cyt f localized on three polypeptides (Joliot and Joliot, 1986). Another protein not associated with redox activity has been shown to be the site of plastoquinol binding (Doyle et al, 1989). Hurt and Hauska (1982) have suggested other small polypeptides to be involved in the complex as well. Several mechanisms have been proposed for the functioning of the cyt b_6f complex, including the Q-cycle (Mitchell, 1975) and the b-cycle (Wikstrom et al, 1981; and others are reviewed in Joliot and Joliot, 1986), though none has been accepted to the exclusion of the other. The controversy arises in that only one eletron traverses the complex for the two protons translocated (i.e. two electrons accepted from plastoquinol). What the models seem to agree on is the division of the redox components into two chains: the FeS center and cyt f, as a pathway to plastocyanin, and the two cyt b_6, as a separate chain. As to which the plastoquinol initially interacts with is not entirely certain but it has been shown that the Rieske protein and its FeS center are essential, not only for the reduction of plastocyanin, but also for the reduction of cyt b_6 (Adam and Malkin, 1987). This suggests that the FeS center may oxidize the plastoquinol and distribute its electrons to the two chains, making it the intermediary between two- and one-electron processes in the cyt b_6f complex.

Plastocyanin is a small, copper containing redox enzyme that loosely binds to the lumen surface of the thylakoid membrane (Droppa and Horváth, 1990). Immunogold labeling experiments have shown that plastocyanin is active in laterally transporting electrons from cyt b_6f sites to PS I in the nonappressed membranes (Haehnel et al, 1989) and further, that reduced plastocyanin can be oxidized by P700 (Wood and Bendall, 1975). More direct evidence has been provided by Hippler et al (1989), in demonstating a specific PS I subunit as the binding site for plastocyanin that provides the conformation necessary for rapid electron transfer to $P700^+$.

The energetic events in PS I immediately preceding the reduction of $P700^+$ by plastocyanin are similar to those in PS II. Excitation energy is transfered to the P700 energy trap from LHC I (Mimuro, 1990). This Chl-a/b containing antennae (Chl-a/Chl-b = 8.0) has quantitatively relatively less chlorophyll but has a more efficient light harvesting capacity than its PS II counterpart (Chl-a/Chl-b = 1.7) due to the lower extinction coefficient of Chl-b relative to Chl-a (Melis, 1989). The nature of P700 itself had been generally been accepted to be a Chl-a dimer (Cogdell, 1988). However, ESR and detail-analysed ENDOR data have dissented in suggesting $P700^+$ to be a monomeric cation radical (reviewed in Golbeck, 1987). In fact, the recent picture seems to indicate P700's neutral ground state to be a dimer but it's excited and triplet states are localized on only

one of the Chl in the loosely coupled pair (Andréasson and Vänngård, 1988; Golbeck, 1987; Cogdell, 1989). Once excited, there follows a charge separation within 2 ps (Evans and Bredenkamp, 1990) involving an intermediate electron acceptor, A_0, which has been indentified as a monomeric specialized Chl a (Lagoutte and Mathis, 1989). The charge is stabilized by a subsequent component, A_1, oxidizing A_0^- in a time of between 32 ps (Shuvalov et al, 1986) and 200 ps (Evans and Bredenkamp, 1990). The identification of A_1 has been tentatively made as phylloquinone (vitamin K_1; Brettel et al, 1986; Itoh et al, 1987) but this is tempered with data that is not readily satisfied with such a characterization (see Lagoutte and Mathis, 1989). Thus, the question is left, according to Hauska (1988), essentially open. Nonetheless, the most recent data is supporting A_1 being indeed phylloquinone (Biggins et al, 1989; Kim et al, 1989; Sétif and Bottin, 1989).

Beyond A_1, electrons are transfered to a series of two iron-sulfur complexes denoted F_X and F_A/F_B. Immediately successive to A_1, F_X has been shown to be a single FeS center composed of a [4Fe-4S] cluster of rather atypical spectrophotometric properties (Scheller et al, 1989; Guigliarelli et al, 1989) and is reduced with a time constant of 200 ns by A_1^- (Evans and Bredenkamp, 1990). However, the pathway and kinetics of electron transfer ensuing from F_X to F_A and F_B are poorly understood (Golbeck, 1987). It is known that the latter centers both are [4Fe-4S]

clusters on a common protein within close distance of each other (Hoj et al, 1987; Wynn and Malkin, 1988), though only weakly coupled by magnetic interaction (Guigliarelli et al, 1989). It is not known if the two centers operate in series or in parallel (Andréasson and Vänngård, 1988), though a linear sequence of F_X -> F_A -> F_B is suggested by their respective redox potentials (Haehnel, 1984). Furthermore, it is not known which of the two is the electron donor to ferredoxin (Golbeck, 1987; Reilly and Nelson, 1988), considered the terminal acceptor of PS I. Ambiguities notwithstanding, once ferredoxin becomes reduced, it can serve as an electron donor to a number of subsequent metabolic enzymes (see below), including ferredoxin:$NADP^+$ oxioreductase, which catalyzes the double reduction of $NADP^+$ to NADPH. The latter enzyme, therefore, serves as the intermediary between the one electron processes of PS I and two-electron reduction (Zanetti and Curti, 1981).

The formation of NADPH reductant is the final step in linear electron transport. However, there are two other pathways for electrons to be shunted, depending on the metabolic demands of the cell: cyclic and pseudocyclic electron transport. The former involves electrons being returned to the cyt b_6f complex from the reducing side of PS I and recycled back to the donor side. Data from the 1960's (Tagawa et al, 1963; Arnon et al, 1964) and 1970's (Arnon and Chain, 1975; Böhme, 1977; Mills et al, 1978) suggested this pathway was mediated by ferredoxin but more recent data

insists that FNR is implicated (Clark et al, 1984; Garab and Hind, 1987; but note that while Clark et al. only showed FNR bound to the cyt b_6f complex, possibly leaving ferredoxin in the actual mediatory role, Garab and Hind demonstrated cyclic flow through FNR in the absence of detectable ferredoxin). It remains uncertain whether cyclic flow is physiologically relevant. To wit, it "has been observed at high rates only in broken chloroplasts supplied with unphysiological cofactors or in the absence of oxygen, (and) does not lead to a gas exchange reaction" (Egneus et al, 1975). The other pathway, pseudocyclic electron flow, involves the reduction of ambient molecular oxygen ultimately to hydrogen peroxide (see below for detailed discussion). This option most certainly occurs in vivo under conditions of maximum carbon fixation and high quantum flux densities (Salin, 1987; Robinson, 1988). Unfortunately, while the reducing side of PS I is definitely implicated, the actual site of the reduction is not clear in the literature. Nonetheless, both ferredoxin and FNR have the potential to reduce dioxygen (Robinson, 1988).

The two alternatives to linear flow have in common the ability to attenuate the formation of NADPH, while maintaining ATP synthesis by virtue of constant proton translocation. However, this reductant is so vital to cellular metabolism (e.g. the Calvin cycle) that they must represent either alternative pathways in the event of the NADP pool being over-reduced or true attenuating pathways to

prevent it from becoming over-reduced in the first place. The basic unresolved question is: given the apparent commensurate metabolic outcome, what is the advantage of one over the other? There is some complementary, though indirect, evidence to indicate the two may occur simultaneously but that cyclic flow is not an alternative to pseudocyclic flow but is coupled to and depends on it to occur at all (Steiger and Beck, 1981; Furbank and Badger, 1983). Also important, is the pivotal role that ferredoxin and FNR may play in the distribution and, ultimately, the fate of electrons acccording to metabolic demands. It is this role that merits a further investigation of the two.

III

It has only been in the last decade or so that researchers have began to bring to light the importance of ferredoxin and FNR in the photosynthetic electron transport chain. Considered individually, the two enzymes are markedly different. Ferredoxin is a nuclear-encoded, iron-sulfur polypeptide (Golbeck, 1987) and considered to be a soluble protein (Zanetti and Curti, 1981; Forti et al, 1983) of about 10 kD. It is also acidic and its 2Fe-2S center is the major force in defining the structure of the protein (Pagani et al, 1986). It has been implicated as an electron donor to several important enzymes including the regulatory enzymes of the Calvin cycle (Wolosuik and Buchanan, 1977), thioredoxin reductase (FTR), sulfite reductase (Zanetti and

Curti, 1981), glutamate synthase (GOGAT; Hirasawa et al, 1989), nitrate reductase (NiR; Hirasawa et al, 1987) and lastly, FNR (Fig. 3). The last is a membrane-bound, flavin-containing enzyme (Golbeck, 1987; Matthijs et al, 1987) of about 33-38 kD (Zanetti and Curti, 1980; Hasumi et al, 1983; Pschorn et al, 1987) that has been shown to have highly specific sites for both ferredoxin and $NADP^+$ (Foust et al, 1969; Sheriff and Herriott, 1981; Karplus et al, 1984).

Considered functionally, a remarkable amount of complementary data strongly supports a cooperative role for ferredoxin and FNR, with the former sourcing electrons from PS I and the latter being an intermediary of one- and two electron processes, as discussed above. Firstly, ferredoxin has been shown to indeed interact at the two sites: the reducing side of PS I and with FNR (Forti and Grubas, 1985). More specifically, cross-linking studies indicate that ferredoxin is bound to PS I by a positively-charged 18 kD peripheral membrane protein (Scheller et al, 1988; Andersen et al, 1990). It is hypothesised that the positive charge aids in overcoming the electrostatic repulsion between negatively-charged ferredoxin and the similarly charged thylakoid membrane surface (Scheller and Moller, 1990). Supporting the cross-linking studies, it was found that a mutant cyanobacteria unable to biosynthesize the 18 kD protein was also unable to photoreduce ferredoxin (Chitnis et al, 1989). Further studies of ferredoxin interaction have shown the formation of a very stable electrostatic complex

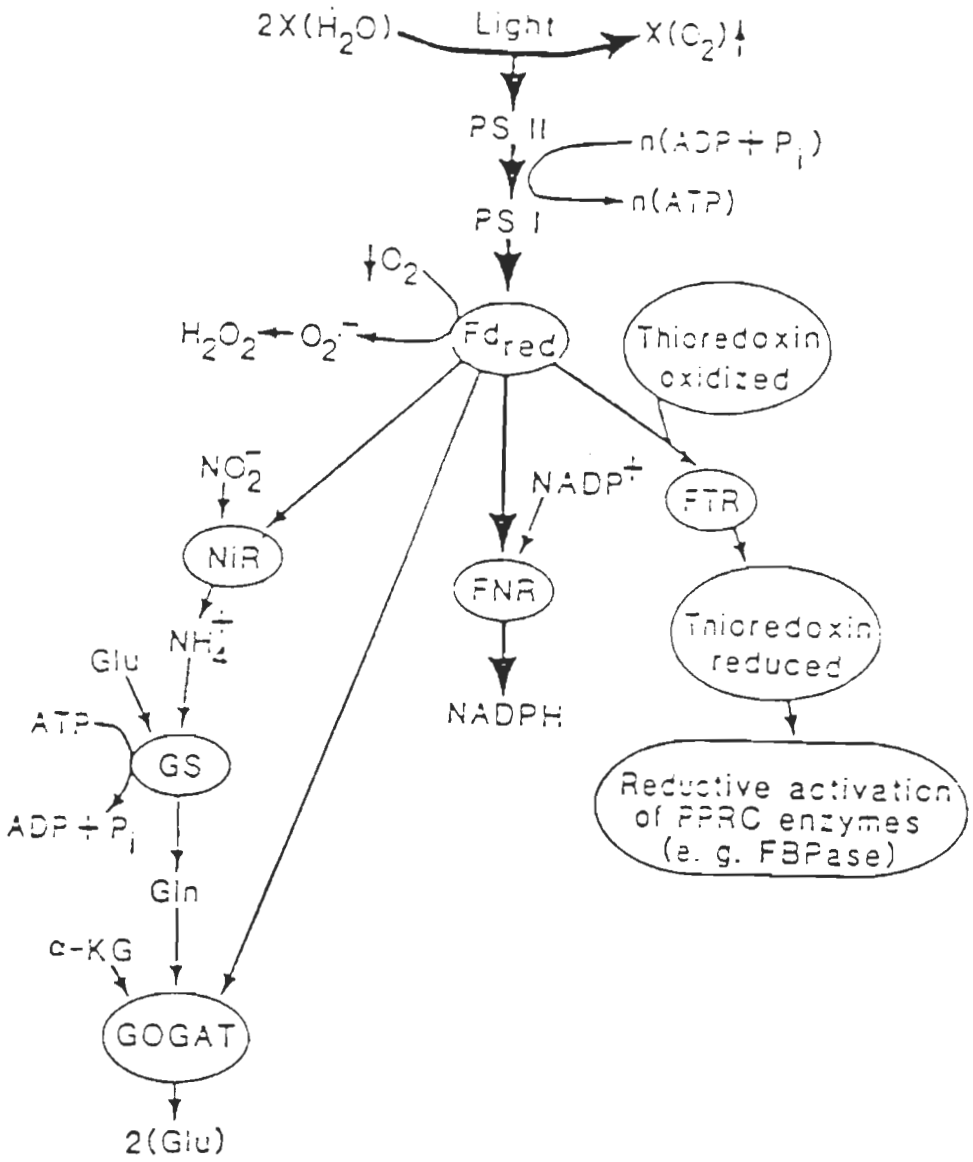

Figure 3. Summary of metabolic reaction sites in which reduced ferredoxin serves as electron donor. Abbreviations as given in the text. (From Robinson, 1988).

with FNR in a 1:1 ratio (Zanetti and Curti, 1981). Though the experiments were performed *in vitro*, the complex was formed irrespective of redox state and required 0.5 M NaCl to separate, suggesting it is entropically highly favoured and would exist *in vivo*. The facts that selective removal of FNR from the thylakoid membrane completely inhibits $NADP^+$ photoreduction but not reduction of ferredoxin by PS I (Forti et al, 1983; Forti and Grubas, 1985) and that ferredoxin is an essential element in $NADP^+$ reduction (Zanetti and Curti, 1981, but Garab et al, 1990 dissent) give further evidence for the *in vivo* complex. However, the complex is not necessarily formed in the stroma, subsequently binding to PS I, as ferredoxin interaction with PS I has been shown to be independent of its binding to FNR (Forti and Grubas, 1985).

Thus, while the roles of the two enzymes have been clearly defined in linear electron transport (Garab et al, 1990, notwithstanding), the involution of their functions in the other electron pathways rests with few clues.

IV

The ablility of oxygen to serve as a photosynthetic acceptor of electrons was originally observed by Mehler (1951) in isolated chloroplasts. The process itself is known as pseudocyclic electron transport or the Mehler reaction and is characterized by oxygen serving as a Hill oxidant and accepting electrons from the reducing side of PS I (Asada

and Takahashi, 1987). Along the Mehler reaction pathway, the reduced oxygen is ultimately converted to hydrogen peroxide. In recent years, the intermediate in the process was shown by many methods to be superoxide ion (Asada and Takahashi, 1987). This ion, considered to possess a small degree of radical character (Sawyer and Valentine, 1981), is produced by PS I within the boundary of the thylakoid membrane, comparatively close to the stromal surface, where it is relatively stable in the prevailing aprotic environment (Takahashi and Asada, 1988). However, once it diffuses to either side of the membrane, it is either spontaneously (in the lumen's acid millieu) or enzymatically (in the stroma) dismutated to hydrogen peroxide by superoxide dismutase (Salin, 1987). As mentioned above, pseudocyclic electron transport virtually certainly occurs *in vivo* under conditions of intense illumination and/or high CO_2 fixation (Egneus et al, 1975; Heber et al, 1978; Robinson, 1988). Further, there is evidence to suggest that it supplies some ATP to drive the Calvin cycle (Halliwell, 1981; Steiger and Beck, 1981) and is capable of balancing the energy requirements of the cell (Furbank et al, 1982). Further support is indirectly provided by the elaborate enzymatic system found in intact chloroplasts to cope with active forms of oxygen (Fig. 4). Catalase, the enzyme most associated with H_2O_2 degradation, is not present in chloroplasts *in vivo* (Halliwell, 1981), unlike superoxide dismutase. Instead, as has been demonstrated by one research

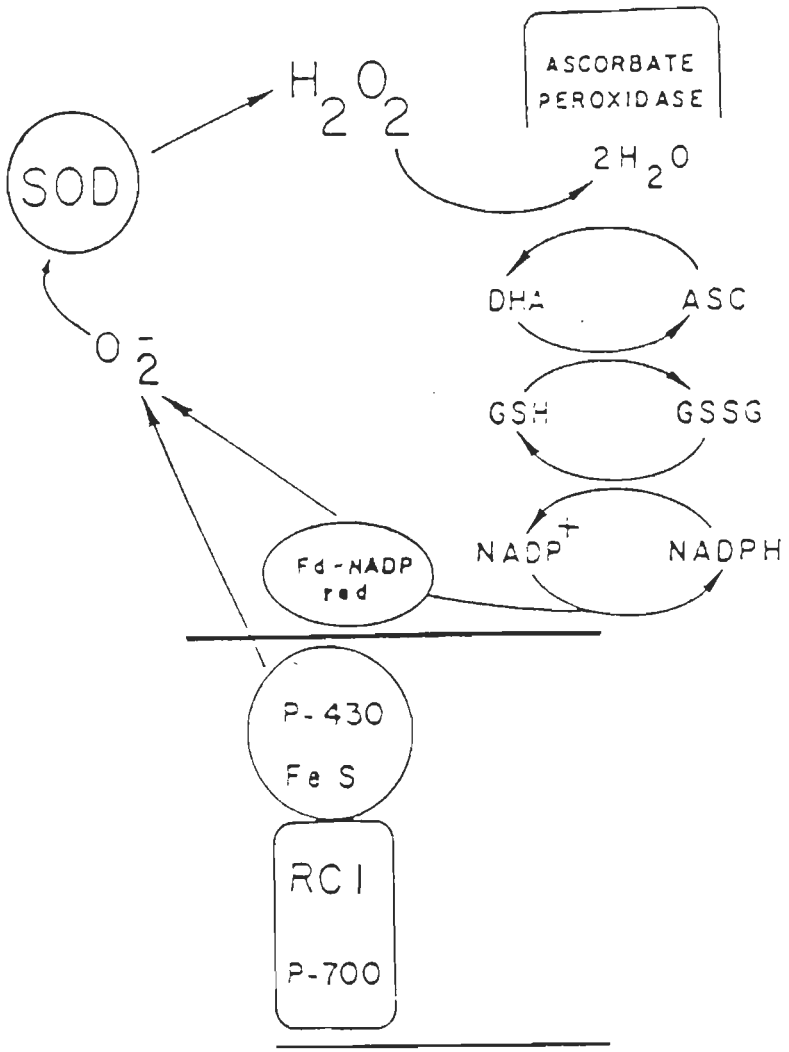

Figure 4. Reaction schema for the endogenous scavenging of hydrogen peroxide in the stroma of chloroplasts. Abbreviations as given in the text. (From Salin, 1987).

team in an elegant series of papers, hydrogen peroxide is scavenged by an ascorbate specific peroxidase, using L-ascorbate (AsA) as substrate (Hossain et al, 1984; Nakano and Asada, 1980, 1981). The reaction products are monodehydroascorbate (MDA) and dehydroascorbate (DHA). The former is converted to the latter by MDA reductase and the latter is recycled to AsA by DHA reductase in a reaction oxidizing reduced glutathione (GSH). Subsequently, glutathione reductase regenerates GSH using NADPH. These results have been confirmed by Jablonski and Anderson (1981, 1982). Thus, not only does pseudocyclic electron transport potentially generate ATP while reducing electron flow to $NADP^+$, it actually consumes NADPH, suggesting it is an attenuating pathway with a role in regulating the redox state of the NADP pool.

The detection of pseudocyclic electron transport usually involves experiments measuring uptake of oxygen manometrically (Mehler, 1951; Good and Hill, 1955), with a Clark electrode (Jennings and Forti, 1974) or using a mass spectrometer in conjunction with labelled (^{18}O) oxygen (Egneus et al, 1975; Marscho et al, 1979; Furbank et al, 1982) in illuminated chloroplasts. The relative merits and difficulties of these varied techniques will be discussed in some detail later in this discourse.

V

Given the ability of the photosynthetic apparatus to induce vectorial electron transport through a chain of redox

species, a properly configured electrochemical cell can be utilized to generate photocurrents and photopotentials from the primary charge separation. More precisely, the photovoltaic effects observed in an electrochemical system are the result of a combination of photophysical, photochemical and electrochemical events. The first involves electronic excitation followed by charge separation, the second deals with reactions of the excited molecules and lastly, the electrochemical step involves charge transfer processes at the interface between the electrolyte and electrode (Gherichер, 1977). Electrodes can be directly involved in exchanging electrons with excited molecules if suitable acceptors and/or donors are in solution or can function as indicators of photo-induced formation of redox couples in solution (Agostiano et al, 1990).

Several electrochemical devices of different architectures have been previously designed to measure photocurrents and photopotentials occuring in the presence of photobiological samples. They employ different strategies of either electrodes covered by films of photosynthetic materials or a suspension of the material, in conjunction with artificial donors/acceptors to mediate interaction with the electrode. In order to familiarize this approach to the study of photosynthesis, a sampling of some of the more recent and innovative eletrochemical cells will be reviewed here, though the list is by no means exhaustive or definitive.

One type of electrochemical cell developed is a virtual in vitro model of the Z-scheme (Agostiano and Fong, 1987). The cell utilizes two platinum foil electrodes with PS II and PS I deposited separately on them (such electrodes had earlier been shown to be viable in Agostiano et al, 1984). So prepared, they are placed in the glass body of the cell, which has three compartments separated by polyacrylamide gel (Fig. 5, above): the first compartment holds the PS II electrode in a buffered solution; the middle one holds a Pt foil counter electrode (for the PS II electrode) and the PS I electrode, immersed in a solution of artificial acceptors (for PS II) and donors (for PS I); the third holds a Pt counter electrode for the PS I electrode in a solution of $NADP^+$. Simultaneously illuminating both electrodes under no imposed potential produced μA anodic currents (though PS I currents were roughly $^1/_4$ those of PS II), a net evolution of oxygen and a reduction of $NADP^+$. This cell represents an excellent potential for studying the Z-scheme through manipulating the separated, individual components.

Another compartmental electrochemical cell has been developed by the Gross laboratory. This cell has but two compartments (Fig. 5, below) and has been used in conjunction with PS I particles (Gross et al, 1978; Pan et al, 1982; Sanderson et al, 1987) and isolated broken chloroplasts (Bhardwaj et al, 1981). The biological sample was deposited onto a porous, cellulose triacetate filter, then placed so as to be the separation between the two

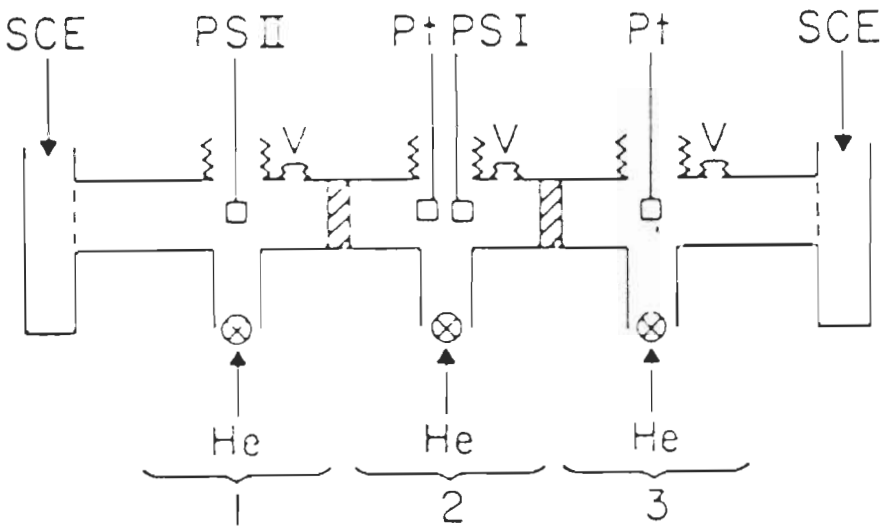

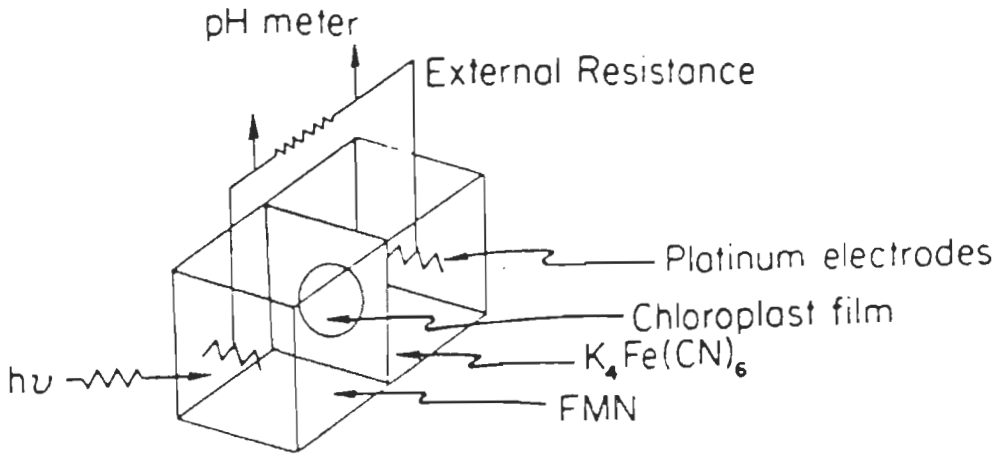

Figure 5. Schematic diagrams of compartmental photoelectrochemical cells. Above, the three chambered cell, separating PS I and II electrodes with polyacrylamide barriers. Below, the two chambered cell where the halves are separated by a PS I-deposited filter. (From Agostiano and Fong (1987) and Gross et al (1978), respectively).

compartments (Fig. 5, below). Both were filled with buffered solutions but one additionally contained an electron donor (e. g. potassium ferricyanide or dichlorophenol indophenol) and the other an electron acceptor (e. g. flavin mononucleotide or phenazine metho- or ethosulfate). Platinum electrodes were immersed in each compartment and connected to a pH meter to monitor voltage. When illuminated through the donor side, the cell's potential has been measured as high as 640 mV with PS I particles and over 500 mV with broken chloroplasts and currents of 15 mA and 4 mA, respectively, were produced under short circuit conditions. The potential generated is in the form of a chemical potential gradient across the cell, by virtue of formation of a strong reductant on one side and a weak oxidant on the other. This is the cell's most important property: the ability to store captured light energy as a chemical potential. However, its configuration restrains the photosynthetic component to suboptimal efficiency compared to the photochemical component, as demonstrated by kinetic factors associated with the reactions. Given the stated goal of divising a source of electric power (as opposed to photosynthetic research as per se), the authors have conceded that the cell needs to be redesigned to allow improvement of the photosynthetic contribution to energy storage by making it independent of the photochemical contribution. Thus, a better understanding of the

photoelectrochemical properties and responses of PS I is needed.

A more unconventional approach has been taken by Greenbaum (1985,1989,1990). Instead of a compartmentalized electrochemical cell, isolated ruptured chloroplasts were metalized by precipitating colloidal platinum onto the surface of the thylakoid membranes. The platinized chloroplasts were then entrapped on fiberglass filter paper and contacted with a platinum gauze electrode. A similar gauze was placed on the other side of the paper to serve as a counter electrode (Fig. 6). Operating in a pure He atmosphere and with no external voltage applied, illumination resulted in nA currents and caused the Pt electrode in contact with the chloroplast to swing negative relative to the counter electrode. This photocurrent orientation is consistent with the model of vectorial photosynthesis presented above and led to the conclusion that the colloidal Pt served as a acceptor to PS I. However, this technology is being pursued more as an energy generation apparatus than an approach to fundamental research.

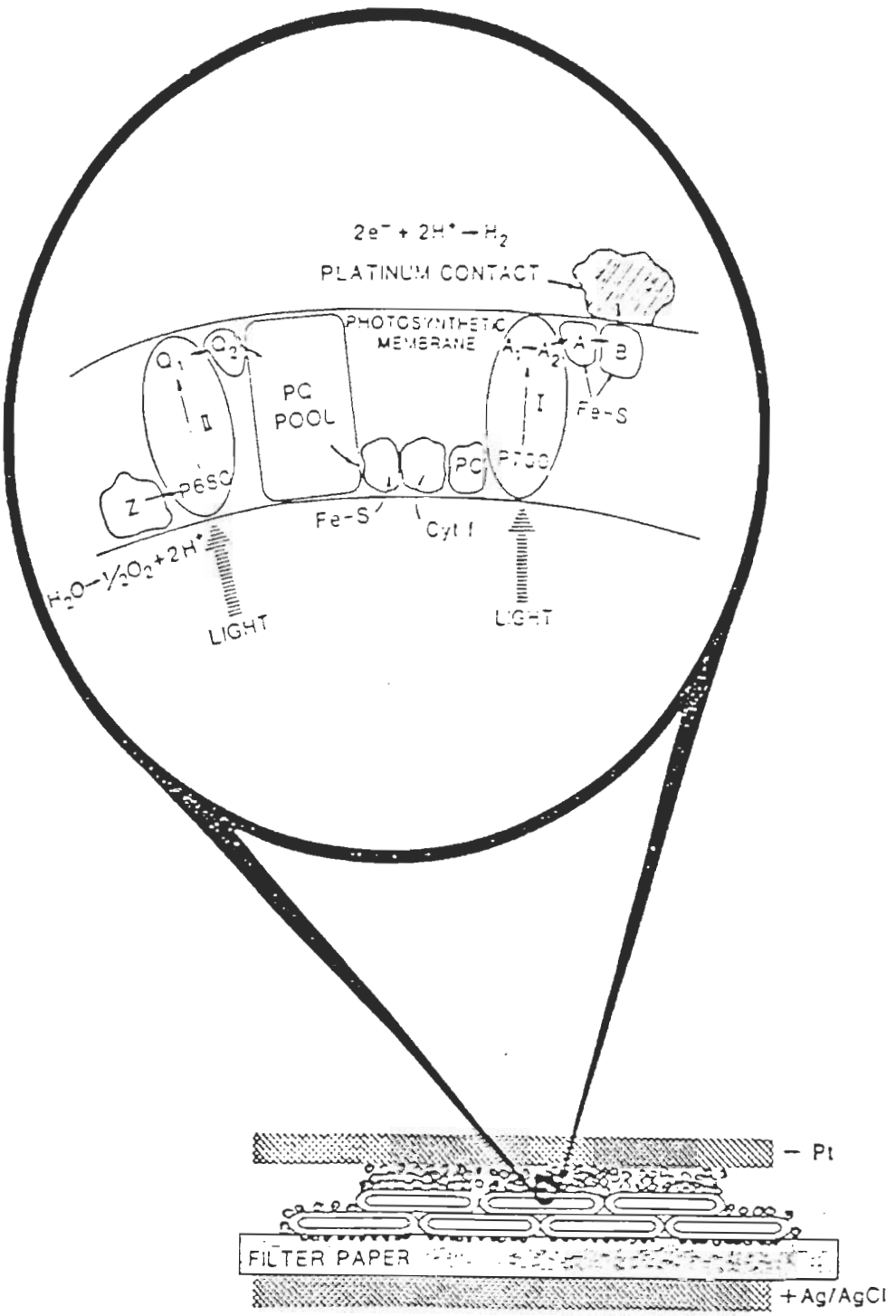

Figure 6. Schematic representation of the platinized chloroplast photoelectrochemical cell. Electrical contact with the reducing end of PS I is made initially by colloidal platinum and, to the larger foil electrode, by metal-to-metal pressure contact. (From Greenbaum, 1989).

MATERIALS AND METHODS

Isolation of thylakoid membranes - Thylakoid membranes were prepared from the deveined leaves of market spinach homogenized in 330 mM sorbitol, 20 mM TES-NaOH pH 7.5 and 5 mM $MgCl_2$. The resulting slurry was filtered through ten (4+6) layers of cheesecloth gauze and the filtrate centrifuged at 4500 x g for 1 min. The supernatant was decanted and the remaining pellet was resuspended in a $^1/_{20}$ dilution of the homogenizing solution. A second centrifugation at 6000 x g for 1 min followed. The supernatant again decanted, the second pellet was resuspended in a solution of 330 mM sorbitol, 50 mM TES-NaOH pH 7.5, 5 mM $MgCl_2$, 1 mM NaCl and 1 mM NH_4Cl. The chlorophyll concentration of the isolated membranes was determined using the acetone extraction method of Arnon (1949) and the thylakoids were diluted to the appropriate experimental concentration, usually 250 $\mu g \cdot mL^{-1}$ in the case of photoelectrochemical measurements. This entire procedure was carried out at 0-4°C and the thylakoids were either used immediately or stored at 77K in liquid nitrogen until needed.

Isolation of PS II-enriched membranes - Membranes enriched in PS II were prepared according to the method of Berthold et al (1981) by homogenizing market spinach leaves in 50 mM Tricine-NaOH pH 7.6, 10 mM NaCl and 5 mM $MgCl_2$ and centrifuging the cheesecloth-filtered (as above) slurry at 4500 x g for 7 min. The supernatant was decanted and the

pellets resuspended in 50 mM Tricine-NaOH pH 7.6, 10 mM NaCl, 5 mM $MgCl_2$ and 0.001 $g \cdot mL^{-1}$ fresh ascorbate. After homogenization, the suspension was recentrifuged at 4500 x g for 7 min and again, the supernatant was decanted. The pellets were resuspended and homogenized in a washing buffer composed of 20 mM MES-NaOH pH 6.2, 15 mM NaCl and 10 mM $MgCl_2$. The Chl concentration of homogenate was determined as above and the sample diluted to a Chl concentration of 1 $mg \cdot mL^{-1}$ with 4 % Triton X-100 in the washing buffer, added very slowly while the mixture was magnetically stirred. After 20 min, the liquid was poured into 2 centrifuge tubes, diluted by ½ again the volume with the washing buffer and centrifuged at 5500 x g for 10 min. The supernatant was decanted to fresh tubes and recentrifuged at 17500 x g for 30 min. The resulting pellets were resuspended and homogenized in the washing buffer and Chl concentration was again determined. Oxygen evolution rates were determined as described below and only samples with strong activity (i. e. 300 $\mu mol\ O_2 \cdot mg\ Chl^{-1} \cdot hr^{-1}$) were further used for experimentation. PS II enriched membranes were always used freshly prepared.

DCBQ preparation - The PS II acceptor DCBQ was dissolved in dimethyl sulfoxide, used at room temperature but protected from exposure to ambient light.

Isolation of PS I-enriched membranes - Spinach membranes enriched in PS I were prepared using digitonin according to the method of Peters et al (1983). Leaves

homogenized in 50 mM Tricine-KOH pH 7.8, 700 mM sorbitol, 10 mM KCl, 10 mM NaCl, 5 mM $MgCl_2$ and 1 mM phenazine methosulfate were filtered through 12 layers of cheesecloth gauze and centrifuged at 3000 x g for 5 min. After decanting, the pellets were resuspended and homogenized in 20 mM Tricine-KOH pH 7.8, 20 mM $MgCl_2$, 1 mM phenazine methosulfate. This was left to incubate several min on ice in the dark, diluted with an equal volume of 20 mM Tricine-KOH pH 7.8, 500 mM sorbitol, 20 mM KCl, 20 mM NaCl and 1 mM phenazine methosulfate and then recentrifuged at 3000 x g for 5 min. Again after decanting, the second pellets were resuspended and homogenized to a Chl concentration of 2 $mg \cdot mL^{-1}$ (determined as above) in a buffer of 20 mM Tricine-KOH pH 7.8 250 mM sorbitol, 10 mM KCl, 10 mM NaCl, 5 mM $MgCl_2$ and 0.2 % digitonin. The mixture was left for 30 min on ice with constant magnetic stirring. Before being centrifuged at 36 000 x g for 30 min the sample was diluted three fold with the same buffer minus digitonin. The supernatant was retained and pooled, followed by centrifugation at 100 000 x g for 60 min. These final pellets were resuspended and homogenized in 20 mM Tricine-KOH pH 7.8, 20 mM NaCl, 20 mM KCl and 5 mM $MgCl_2$ to a CHl concentration of 3.3 $mg \cdot mL^{-1}$ (determined as above). PS I enriched membranes were always used immediately subsequent to preparation.

DQ preparation - The PS I donor tetramethyl-p-benzoquinone (duroquinone) was dissolved in 1:1

ethanol/ethylene glycol and reduced according to the method of Izawa and Pan (1978). Thus, 2 mg $NaBH_4$ was added to 1 mL dissolved DQ and the mixture was vigorously mixed. After sitting 5 min, 5 µL HCl (conc) was added to stabilize the hydroDQ and decompose any remaining $NaBH_4$. So prepared, DQ was protected from light exposure and used at room temperature.

Electrochemistry, the photoelectrochemical cell - The photoelectrochemical cell (PEC) used is a modified version of the design originally proposed by Allen and Crane (1976). As shown in Figure 7, it consists of a stainless steel base and a plexiglass cover, separated by a 1 mm thick rubber gasket. The rubber gasket has a 1 cm-diameter hole in its middle constituting the cell chamber. The three are tightly secured together with four screws and, assembled, the chamber has a volume of 80 µL. The chamber is filled via a small diameter channel connecting to a 4 mm opening in the cover. It is evacuated via a 3 mm opening immediately superior to the chamber.

The PEC functionally operates with a three electrode system. A flat, platinum (0.025 mm thick 99.99 % Pt foil, Johnson Matthey Electronics) working electrode is positioned between the base and gasket, covering the entire surface area of the chamber. Between the gasket and cover is positioned a platinum (0.05 mm thick) counter electrode, projecting only a corner into the chamber. Finally, a standard calomel electrode (Fisher Scientific Co., porous

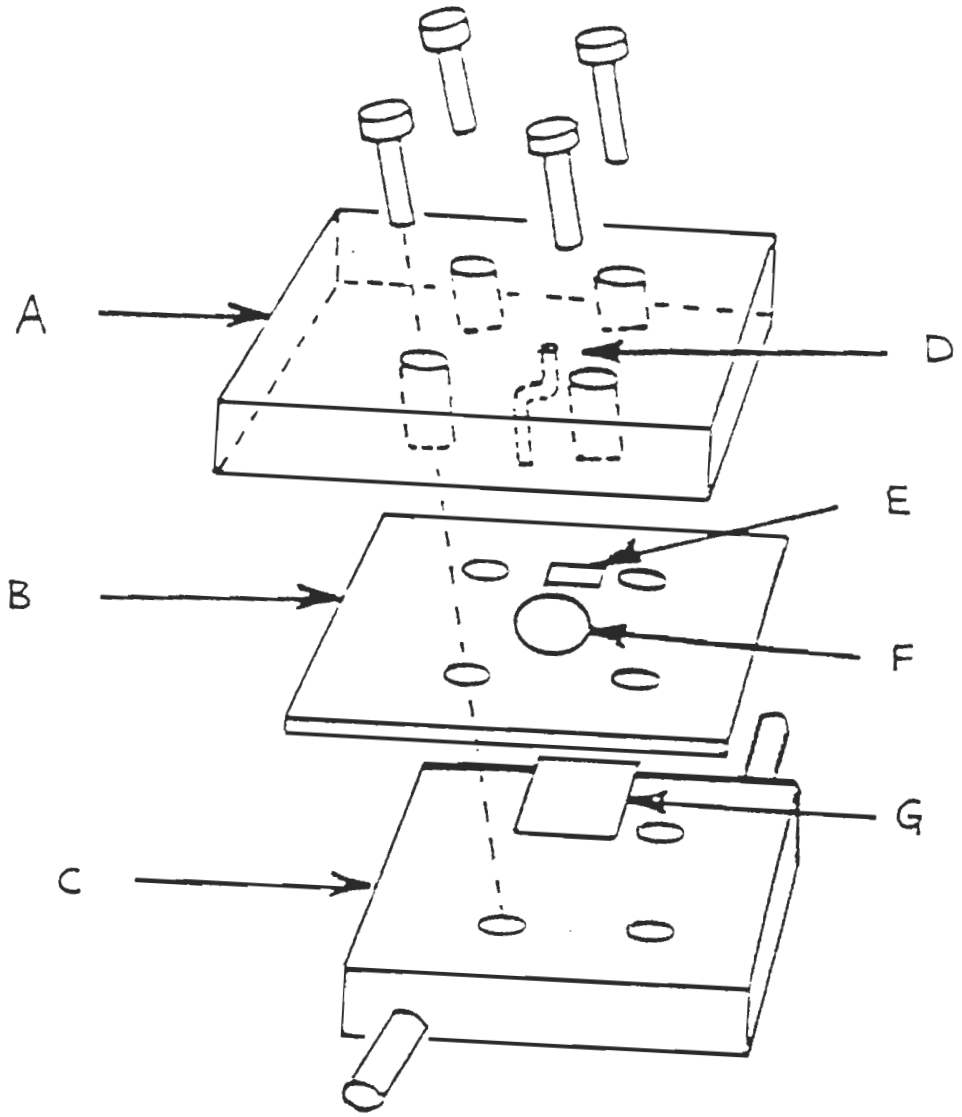

Figure 7. Schematic of unichambered photoelectrochemical cell. A, plexiglass cover; B, rubber gasket; C, steel base; D, filling channel and reference electrode contact site; E, platinum counter electrode; F, 80 µL sample chamber; G, platinum working electrode.

plug type, # 13-639-51) is inserted into the 4 mm opening in the circuit to apply and maintain potential. A standard redox couple (ferri/ferrocyanide) was used in order to control the system. A reversible, diffusion-controled current was monitored. The potential of ferricyanide was shifted by about 100 mV in comparison with standard values reported in the literature (Bard and Faulkner, 1980) because of the high internal resistance and the particular design of the cell (i.e. the relatively distant placement of the reference electrode compared to the two others) that does not allow complete compensation of the IR drop across the distance between the platinum electrodes.

The PEC is illuminated by white light (220 $mW \cdot cm^{-2}$ at the cell chamber) from a 250 W quartz halogen source directed onto the top of the cell by a glass fibre optic guide. The temperature was controlled at 22°C by a Haake AG model A80 thermostated water bath circulating water through the base of the cell.

Electrochemistry, potentiostatic operation - When operated potentiostatically, the cell was connected to an EG&G PARC Model 362 scanning potentiostat working in conjunction with a Linear Co. model 555 chart recorder. A constant potential of 750 mV was applied to the PEC and a 3 min equilibration period was allowed before illumination of the sample.

Electrochemistry, cyclic voltammmetry - To obtain cyclic voltammetry curves for thylakoid membranes, the PEC

was connected to an EG&G PARC model 273 potentiostat/galvanostat. Separate scans were performed with potential ranging from -300 to 1000 mV for samples in the dark and illuminated samples. Oxidation curves were always measured first, followed immediately by reduction curve return scans. Initial potential was applied and scans initiated after a 30 s delay. Results were recorded on a Recorder Co. model 200 X-Y recorder.

Oxygen evolution - Measurements of oxygen evolution/uptake were performed using a water-jacketed Clark-type electrode maintained at 22°C. Thylakoid membrane samples at a concentration of 250 $\mu g \cdot mL^{-1}$ were measured in the homogenization solution described above. Samples were illuminated at an intensity of 75 $mW \cdot cm^{-2}$ by a Fiber-Lite high intensity projection lamp after a short equilibration period. Oxygen consumption was allowed to occur for 1 min when illumination was turned off and 1000 $units \cdot mL^{-1}$ catalase was injected into the sample by Hamilton syringe. This resulted in opposite slope oxygen evolution, directly corresponding to the oxygen consummed by PS I and free of background PS II oxygen evolution.

Spectroscopy, absorption spectra - Samples of 10 μg $Chl \cdot mL^{-1}$ had absorption measured on a Perkin-Elmer model 553 FastScan UV/Vis spectrophotometer manipulated by a Perkin-Elmer model 3600 data station. The spectrophotometer slit was set at a width of 1.0 nm. Data was measured over a range of 420 - 720 nm at 1 nm intervals and at a rate of 120

$nm \cdot min^{-1}$. Response time was 0.5 s. Spectra were recorded on a Perkin-Elmer model R100 chart recorder.

Spectroscopy, action spectra - The action spectra of thylakoid membranes were obtained using the PEC connected to a home-made potentiostat imposing a potential of -140 mV vs SCE in the case of thylakoid- and PS II enriched membranes and 0 mV vs SCE for PS I enriched membranes. The difference in potential relative to potentiostatic measurements was due to limitations of the home-made potentiostat (it could not reliably impose potentials higher than + 300 - 350 mV vs SCE). Therefore, photocurrent signals were optimized from a range of lower potentials and the above-mentioned potentials represent the optimal photocurrent generation of each type of membrane. Samples were measured at a concentration of 10 $\mu g \cdot mL^{-1}$ to avoid the light scattering effects, manifested as a distorted spectrum, observed at higher concentrations. Samples were illuminated by fibre optic guide (as above) with light from 720-420 nm provided by an Applied Photophysics f3/4 monochrometer with a stepping motor control unit. The light source was an ICL Technologies bulb powered with 9 A DC lamp current by an ICL Technologies model Illuminator power source. Exposure time was regulated by an Ilex Optic Co. No. 1 synchro electronic shutter and was optimized at 4 s exposure and 1 s dark interval. The entire apparatus was interfaced and controlled by an IBM PS/2 PC model 30 running "Photoelectrochemistry, version 4.3" developed by A. Paquette, A. Tessier and Dr. P. F.

Blanchet. Spectra obtained were corrected for the lamp emission spectrum and filtered to smooth curves.

Isolation of ferredoxin - The procedure of Yocum et al. (1975) was used to isolate pure ferredoxin from spinach leaves. Approximately 2 kg of washed, deveined market spinach leaves were homogenized in 2.5 L of a 0.02 M Tris (pH 8.0) buffer containing 0.4 M sucrose and 0.015 M NaCl. The homogenate was passed through 4 layers of cheesecloth gauze and centrifuged at 1000 x g for 2 min, after which the supernatant was collected and recentrifuged at 5000 x g for 10 min. The accumulated supernatants yielded about 2.7 L of pale green, opaque liquid. To this was added 8 L of -20° C acetone during continuous magnetic stirring to precipitate the proteins in solution. The stirring was continued several min before allowing the resulting precipitate to settle for 30 min. At the end of this period, 80 % of the acetone was removed by vacuum suction and the precipitate was resuspended in the remaining solvent by gentle swirling. The suspension was then centrifuged for 5 min at 4000 x g and the supernatant decanted. A 0.1 M Tris (pH 8.0) buffer was used to resuspend the pellets and this suspension was homogenized in a homogenization tube, followed by centrifugation at 20 000 x g for 10 min. The collective supernatants totaled approximated 450 mL and were dialyzed in membrane tubing with a 6 000 - 8 000 molecular weight exclusion limit against 10 volumes of 0.05 M Tris (pH 8.0) for 12 hr to remove residual acetone. The solvent-free

protein solution had solid NaCl added to it to a concentration of 0.2 M and was loaded onto a 3 x 60 cm DEAE-cellulose chromatography column equilibrated with 0.05 M Tris (pH 8.0) and 0.2 M NaCl. The resulting dark brown band was washed with 0.5 M Tris (ph 8.0)-0.25 M NaCl, causing the band to start migrating. True elution was effected by 0.05 M Tris (pH 8.0)-0.8 M NaCl. The eluate was treated with 0.6 g/mL ammonium sulfate, maintaining pH 8.0 by adding several drops of unneutralized 1.0 M Tris. The treatment produced a precipitate of unwanted protein that was allowed to settle for 30 min and was then removed by centrifugation at 10 000 x g for 15 min. The pooled supernatants were dialyzed in membrane tubing as above for 12 hr against 40 volumes of 0.05 M Tris (pH 8.0), with the buffer renewed after 6 hr. Now exempt of ammonium sulfate, the remaining protein (now impure ferredoxin) was loaded onto a second 3 x 60 cm DEAE-cellulose column, equilibrated with 0.05 M Tris (pH 8.0), and moved down to the lower $^{1}/_{3}$ of the column by washing with 0.05 M Tris (pH 8.0)-0.2 M NaCl. The flow was stopped and the upper $^{2}/_{3}$ of the colunm was then removed by vacuum suction to accelerate the elution after increasing the buffer's ionic strength. Once the gel had resettled and a smooth top surface was acheived, flow was reinstated and the protein eluted with 0.05 M Tris (pH 8.0)-0.35 M NaCl. Analyzed spectrophotometrically, the pure ferredoxin was found to have a A_{420}/A_{276} ratio of > 0.48 and a spectrum characteristic of oxidized ferredoxin (Fig. 8), as compared

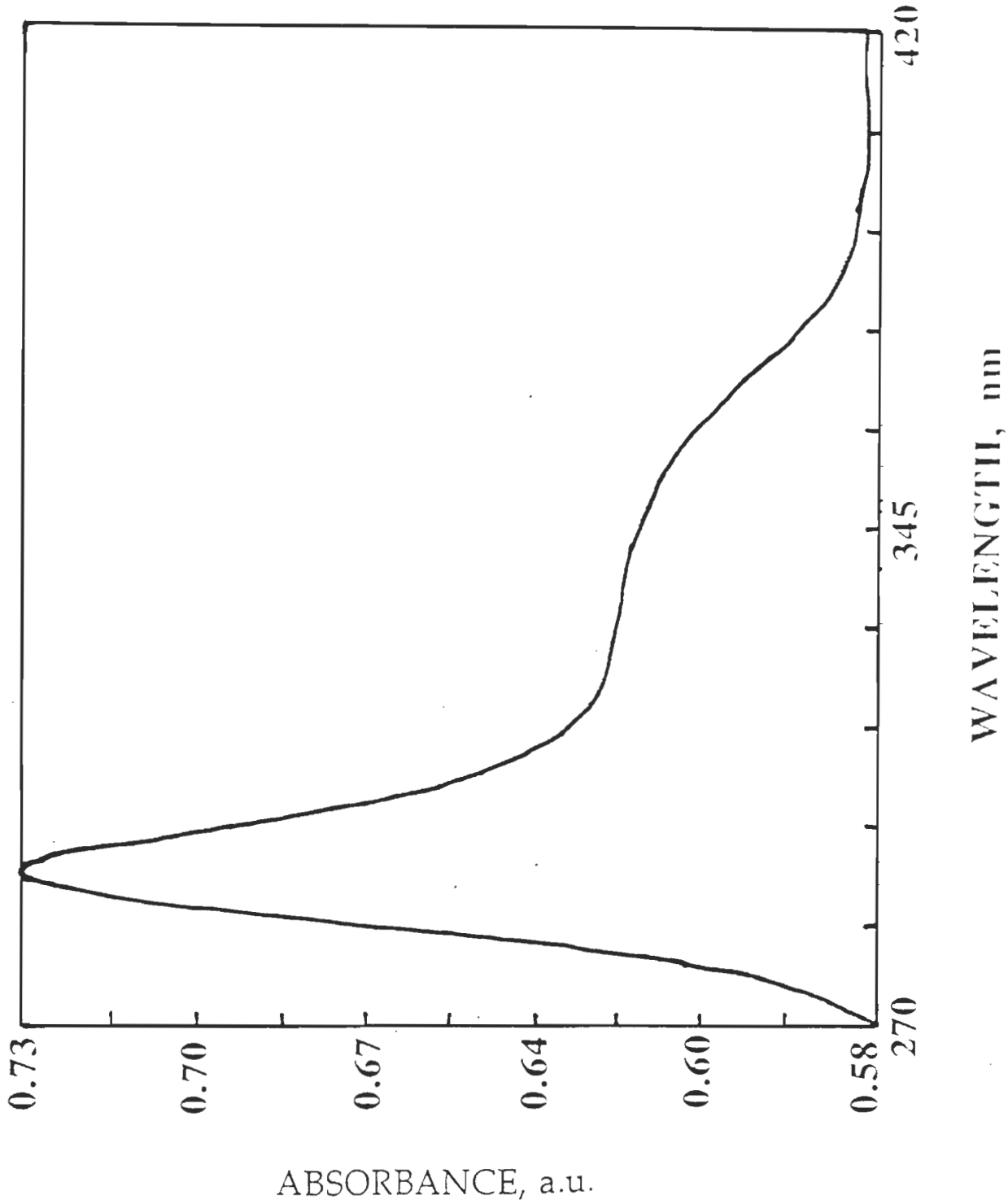

Figure 8. Absorption spectrum of biochemically isolated spinach ferredoxin. This spectrum is consistent with the oxidized state of ferredoxin, as shown in the literature (Buchanan and Arnon, 1971)

to the literature (Buchanan and Arnon, 1971). Concentration was determined using Beer's law based on A_{420} absorbance and a molar extinction coefficient of 9.7 $mg \cdot mL^{-1}(cm^{-1})$ (Buchanan and Arnon, 1971). Purity was also verified by electrophoresis gel chromatography, described immediately subsequent.

Electrophoresis - The purified ferredoxin extract and a commercially obtained "ferredoxin" product were analyzed by sodium dodecyl sulfate polyacrylamide gel electrophoresis (SDS-PAGE) using a Pharmacia LKB Biotechnology PhastSystem unit. This highly automated system uses pre-made gels - PhastGel Gradient 10-15 - with dimensions of 50 mm x 43 mm x 0.45 mm, composed of a 13 mm stacking zone and a 32 mm continous 10 - 15 % gradient zone having 2 % cross linking. The gel is buffered with 0.112 M acetate and 0.112 M Tris (pH 6.4). The running buffer, in the form of a 2 % agarose IEF solid strip, consisted of equimolar quantities 0.2 M tricine and Tris (pH 8.1), as well as 0.55 % SDS (analytical grade). Once "assembled" the gel electrophoresis is fully automatic. Samples were electrophoresed against Bio-Rad molecular weight standards (range: 10 000 - 100 000 Da) consisting of phosphorylase, bovine serum albumin, ovalbumin, carbonic anhydrase, soybean trypsin inhibitor and lysozyme. The standards are supplied as a 2 $\mu g \cdot \mu L^{-1}$ suspension in 50 % glycerol.

The gel was stained with Coomasie brilliant blue after being transfered to the Development Unit of the apparatus.

The unit, also fully automated, uses a fixing solution of 20 % trichloroacetic acid, a washing/destaining solution of 30 % methanol, 10 % acetic acid and distilled water mixed 3:1:6 (v:v:v) and a staining solution of 0.02 % PhastGel Blue R in 30 % methanol and 10 % acetic acid in distilled water (again 3:1:6) and 0.1 % $CuSO_4$ (w/v). Finished gels were analyzed using an LKB-Bromma Ultrascan XL Enhanced Laser Densitometer interfaced with a microcomputer.

Addendum: A brief list of products used - The following provides a partial listing of the products used during the course of the experiments performed, the supplying company and the quality, where available.

1) Buffers -

TES, N-tris[hydroxymethyl]methyl-2-aminoethanesulfonic acid: Sigma Chem. Co., grade not specified (gns).

Tricine, N-tris[hydroxymethyl]-methylglycine: Sigma Chem. Co., gns.

Tris, tris[hydroxymethyl]aminomethane (commercial name, Trizma): Sigma Chem. Co., reagent grade.

Sorbitol, D-glucitol: Sigma Chem. Co., gns.

Sucrose: Fisher Scientific Co., ultra centrifugation grade.

2) Enzymes -

Catalase, from bovine liver: Sigma Chem. Co., thymol-free purified powder.

Ferredoxin, from spinach: Sigma Chem. Co., lyophilized powder, containing approx. 25% ferredoxin, balance

reported as trizma buffer (but see Results and Discussion).

Glucose oxidase, from Asperigillus niger, type II-S: Sigma Chem. Co., product approximately 20 % pure, balance being potassium gluconate.

Superoxide dismutase, from bovine erythrocytes: Sigma Chem. Co., product approximately 98 % pure, balance being primarily potassium phosphate buffer salts.

3) Salts -

Ammonium chloride, NH_4Cl: Sigma Chem Co., gns.

Magnesium chloride, $MgCl_2$: Sigma Chem Co., gns.

Sodium chloride, NaCl: Fisher Scientific Co., enzyme grade.

Methyl viologen, 1,1'-dimethyl-4,4'-bipyridinium dichloride: Sigma Chem. Co., gns.

ß-Nicotinamide adenine dinucleotide phosphate, $NADP^+$: Sigma Chem. Co., approx. 98 % pure (preparation dependent).

4) Miscellaneous -

Acetone: Anachemia (Canada) Co. Ltd., 99.5 % pure.

DEAE-cellulose (commercial name, DEAE-Sephacel): Pharmacia LKB Biotechnology AB, pre-swollen in 20 % ethanol.

2,5-Dichloro-p-benzoquinone, DCBQ: Eastman Kodak Co., gns.

Digitonin: Sigma Chem. Co., approx. 50 % pure.

Tetramethyl-p-benzoquinone, Duroquinone: Sigma Chem. Co., gns.

Triton X-100, octyl phenoxy polyethoxyethanol: Sigma Chem Co., gns.

RESULTS AND DISCUSSION

I

The photocurrent generated by whole thylakoid membranes in the photoelectrochemical cell operating under potentiostatic conditions is shown in Fig 9A. The magnitude of the photocurrent obtained without the addition of exogenous electron acceptors consistently ranged between 4 and 7 μA, depending on the preparation used. Figure 9D shows the effect of 10 μM DCMU, a competitive inhibitor of PS II at the site of QB (Pfister and Arntzen, 1979; Kyle, 1985). The photosynthetic origin of the photocurrent generated is demonstrated by the strong inhibitory effect of DCMU. The remaining photoactivity is a result of a measurable photoeffect between the strong illuminating light and the platinum working electrode. It is observed even with the photoelectrochemical cell working in the absence of thylakoids and produces traces similar in magnitude to the one shown in Fig 9D.

There are two possible hypotheses to explain the generation of strong photocurrents by the thylakoid membranes, both processes involving oxygen. In the first process (Fig. 10, above), the excited photosystems adsorbed on the surface of the platinum electrode could exchange electrons directly with the electrode itself and be subsequently reduced by a donor in solution. In the absence of exogenous donors, this role would be performed by water. On the other hand, the second process would involve the

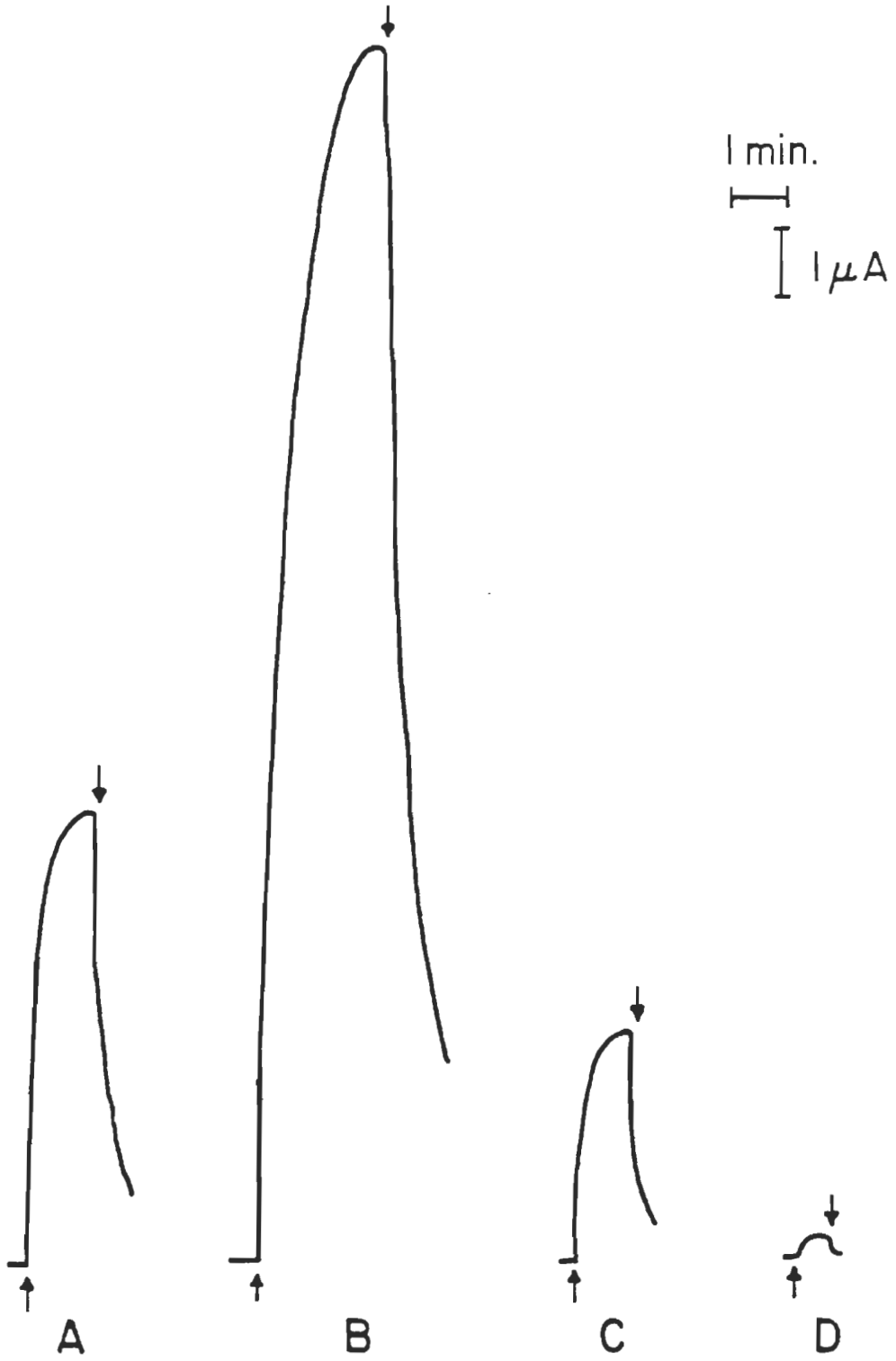

Figure 9. Photocurrent generation by thylakoid membranes (Chl conc. = 250 $\mu g \cdot ml^{-1}$) in the photoelectrochemical cell operating potentiostatically (+750 mV vs. SCE). A, membranes alone; B, with 10 μM methyl viologen; C, bubbled with N_2 gas; D, with 10 μM DCMU. Up and down arrows indicate light on and off, respectively.

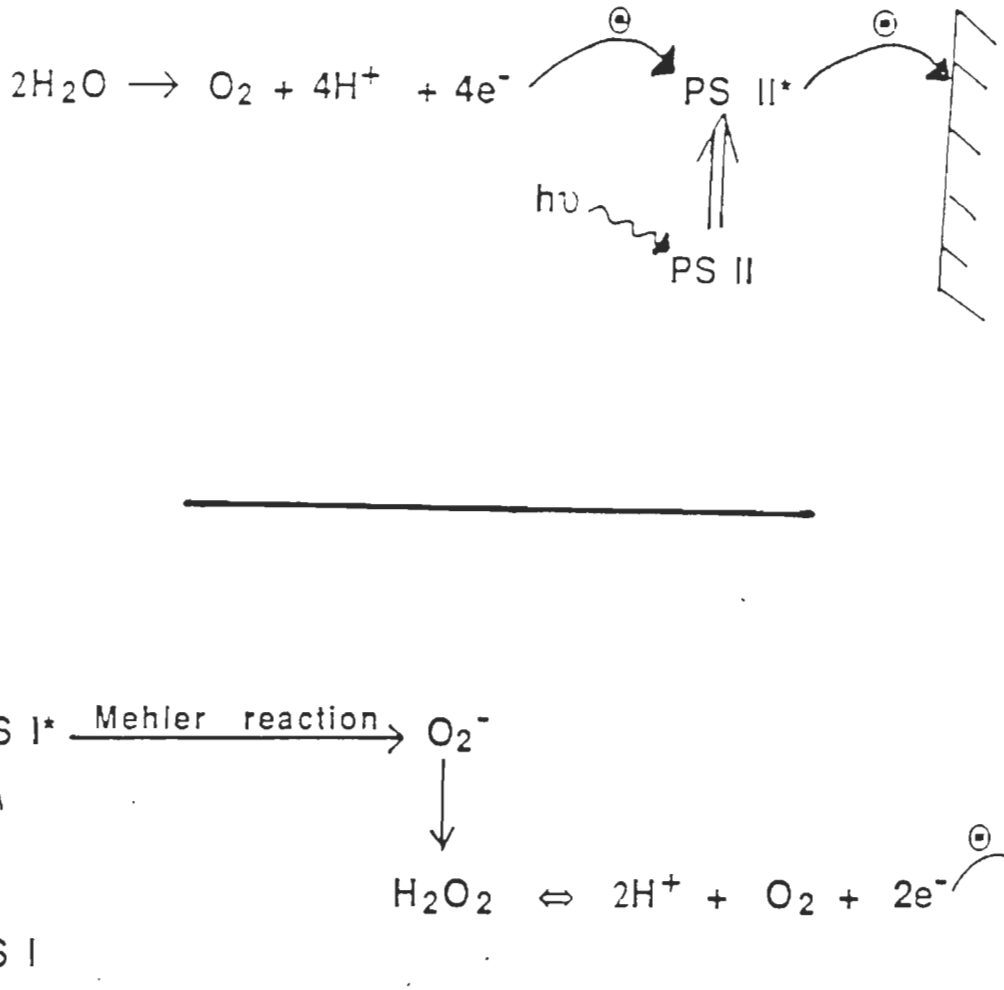

Figure 10. Two potential mechanisms for the generation of photocurrent. Above, electrons are passed directly to the working electrode by photosystems in contact with it; below, electrons are mediated to the working electrode by a preceding chemical reaction, the Mehler reaction.

uptake of oxygen by PS I, following along a Mehler reaction pathway. Thus, photocurrent would be due to the oxidation of hydrogen peroxide at the electrode and its magnitude, in direct proportion to the quantity of H_2O_2 reacting. In this case, the electrode works as an indicator of a photochemical reaction in solution, as shown in Fig 10, below. The effect of methyl viologen on photocurrent generation would lend initial support to the latter hypothesis. This compound has been shown to be an exclusive electron acceptor of PS I whose reduced form will univalently reduce ambient oxygen and is further known to accelerate a Mehler type reaction (Izawa, 1980). Its addition to thylakoids causes a large increase in photocurrent (Fig. 9B), typically 180-220 %. Further supporting the hypothesis, if dissolved oxygen is displaced by bubbling nitrogen gas through the sample before photoelectrochemical measurements are taken, photocurrents are reduced on the order of 50 % (Fig. 9C) relative to untreated thylakoids.

Based on these initial indications, the technique of cyclic voltammetry was employed to identify the electroactivity of oxygen species implicated in the photocurrent. The behavior of oxygen at a smooth platinum electrode has been the object of constant research; its evolution from water, to give PtO, gives rise to two peaks (Tarashevich and Radyushkina, 1970) corresponding to the reactions:

$$H_2O + Pt \rightarrow (Pt)OH^{\cdot}_{ads} + H^+ + e^- \qquad (1)$$

$$(Pt)OH^{\cdot}_{ads} \rightarrow PtO + H^{+} + e^{-} \qquad (2)$$

and its reduction can proceed by two different steps (Koryta et al, 1970) corresponding respectively to:

$$O_2 + 2H^{+} + 2e^{-} \rightarrow H_2O_2 \qquad (3)$$

$$H_2O_2 + 2H^{+} + 2e^{-} \rightarrow 2H_2O \qquad (4)$$

If PtO is formed, its reduction proceeds quickly toward the formation of water. The inset of Figure 11 shows the cyclic voltammetric current-potential curves of a smooth platinum electrode. As expected (Bard and Faulkner, 1980), the peaks respectively corresponding to the formation of a platinum oxide layer (O_A), the beginning of oxygen evolution from bulk water electrolysis (O_B) and the reduction of the adsorbed oxygen (O_C) are clearly in evidence. In the photoelectrochemical cell, the presence of unilluminated thylakoid membranes (Fig. 11A) results in a relevant inhibition of the current due to the formation of adsorbed oxygen, perhaps due to the adsorption of thylakoids on the surface of the electrode. Accordingly, the corresponding peaks are now poorly displayed in the polarographic curve. However, the illumination of the thylakoid sample (Fig. 11B) is marked by the appearance of a strong photocurrent, starting at a potential greater than 250 mV. The current-potential curve no longer shows a peak in the region of oxygen formation and the photocurrent tends toward the limiting value of 20 μA, which remains constant until the bulk oxygen evolution starts. The flat polarographic wave observed is characterized by a half-peak potential (more

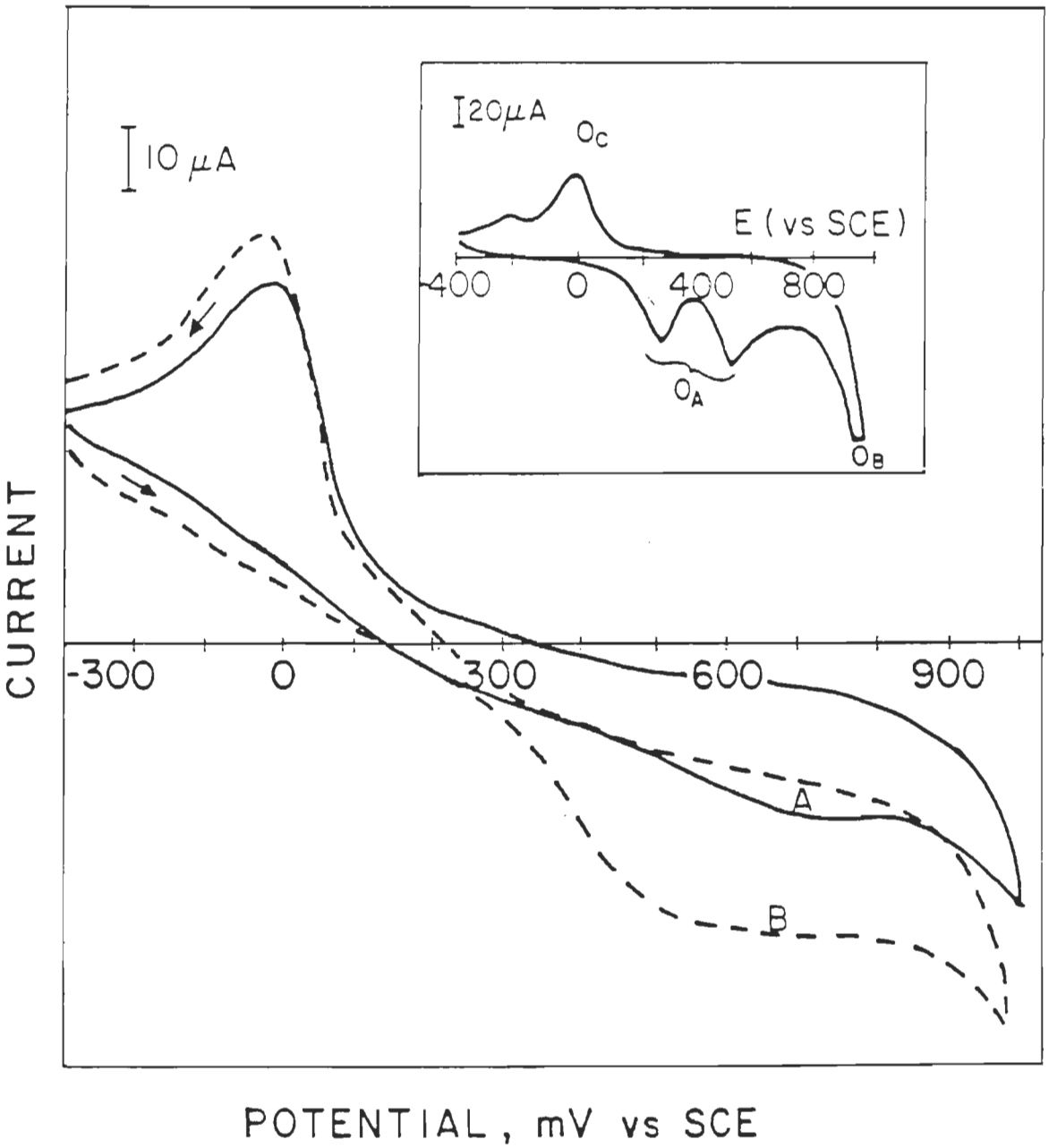

Figure 11. Cyclic voltammograms of thylakoid membranes (Chl conc. = 250 $\mu g \cdot ml^{-1}$). A, unilluminated; B, illuminated. Inset: cyclic voltammo-gram of the buffer solution at the platinum electrode. Scan speed = 10 $mV \cdot s^{-1}$.

convenient to use than the peak potential when a current plateau is observed) of 380 mV. Furthermore, the data summarized in Table 1 shows the photocurrent independent of scan rate up to 20 $mV \cdot s^{-1}$ but dramatically decreases when the scan rate reaches values of 50 $mV \cdot s^{-1}$ or greater.

These data firmly reinforce the oxygen uptake hypothesis for several reasons. First of all, the anodic photocurrent is no longer shaped as a peak but as a flat wave, indicating that a process other than reactions (1) and (2) is taking place. Moreover, the presence of a constant limit photocurrent evinces a preceding chemical reaction is coupled with the electrode reaction (Bard and Faulkner, 1980). If the dependence of the value of $E_{p/2}$ on the scan rate is plotted (Fig. 12), the resulting straight line, with a slope of 17 mV, allows the calculation of the number of electrons involved in the electrochemical process, using the equation (Bard and Faulkner, 1980):

$$\frac{d\ Ep/2}{d\ \ln V} = \frac{R\ T}{2nF}$$

where, R is the gas constant, T is temperature (K), n is the number of electrons and F is Faraday's constant. The solution shows that two electrons are involved and it is reasonable to assume that the photocurrent is due to the reduction of the electrode by hydrogen peroxide as per reaction (4). In turn, the peroxide is continuously provided at the electrode by the preceding uptake of oxygen by PS I.

Table 1. Photocurrent generated by thylakoid membranes during cyclic voltammetry at various scan speeds. Scans were performed from -300 mV to 1000 mV imposed potential. Photocurrents were measured at 500 mV.

SCAN SPEED ($mV \cdot s^{-1}$)	PHOTOCURRENT (μA)
5	20.0
10	18.0
15	19.0
20	17.5
50	3.5

Figure 12. Plot of half-peak potential values ($E_{p/2}$) of the oxidation curves recorded with illuminated thylakoid membranes against the natural logarithm of the scan rate (v) used to obtain the voltammograms.

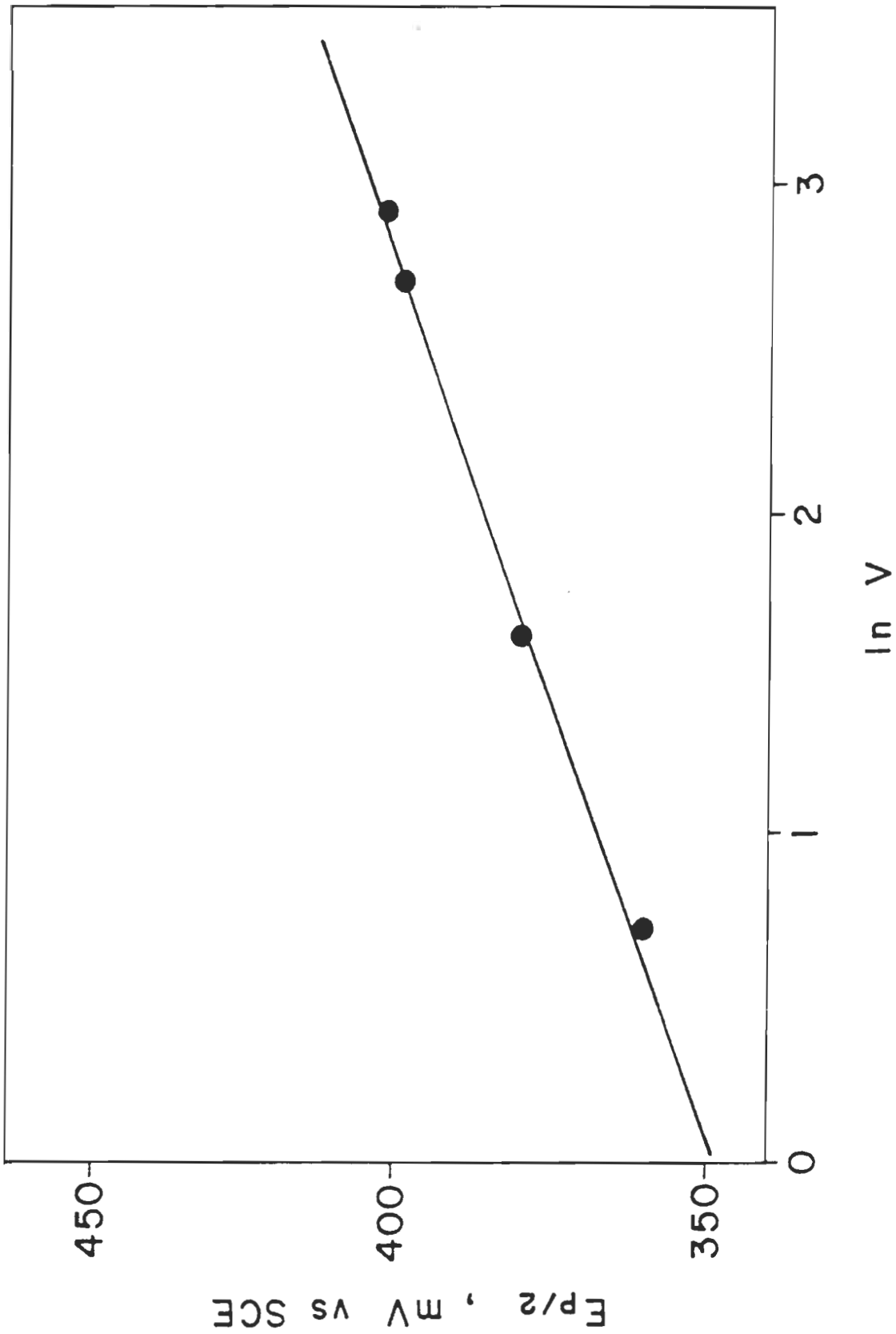
450
400
350
$E_{p/2}$, mV vs SCE
0
1
2
3
ln V

The concomitant supply of oxygen by the OEC of PS II can account for the steady behavior of the photocurrent.

Figure 13 shows the inhibition of photocurrent production by the three enzymes glucose oxidase, superoxide dismutase and catalase. Glucose oxidase produces an intermediary inhibitory effect relative to the other two, an attenuation consistent with a previous report (Mimeault and Carpentier, 1989). When added with a small amount of glucose, this enzyme removes dissolved oxygen during the course of its reaction and thus, its inhibition redundantly implicates oxygen's role in the photocurrent. Since the immediate product of oxygen reduction by PS I is superoxide, the photocurrent should be inhibited by superoxide dismutase. In fact, this enzyme did inhibit, though only poorly, with less than 40 % inhibition in the presence of 1500 units$\cdot mL^{-1}$. The enzyme's action does not change the overall oxygen stoichiometry of the superoxide dismutation reaction relative to proton-induced dismutation but accelerates the resulting formation of peroxide (rate constant for the latter is 10^5 $M^{-1}\cdot s^{-1}$ vs. 2×10^9 $M^{-1}\cdot s^{-1}$ for the enzymatic process). As it has been shown that the production of photocurrent is limited by diffusion (Mimeault and Carpentier, 1989), such a sudden concentration increase leaves some peroxide molecules free to participate in other reactions, damaging the thylakoids. In fact, hydrogen peroxide is well known to inhibit photosynthesis at elevated concentrations thus, the weak inhibition of photocurrent by

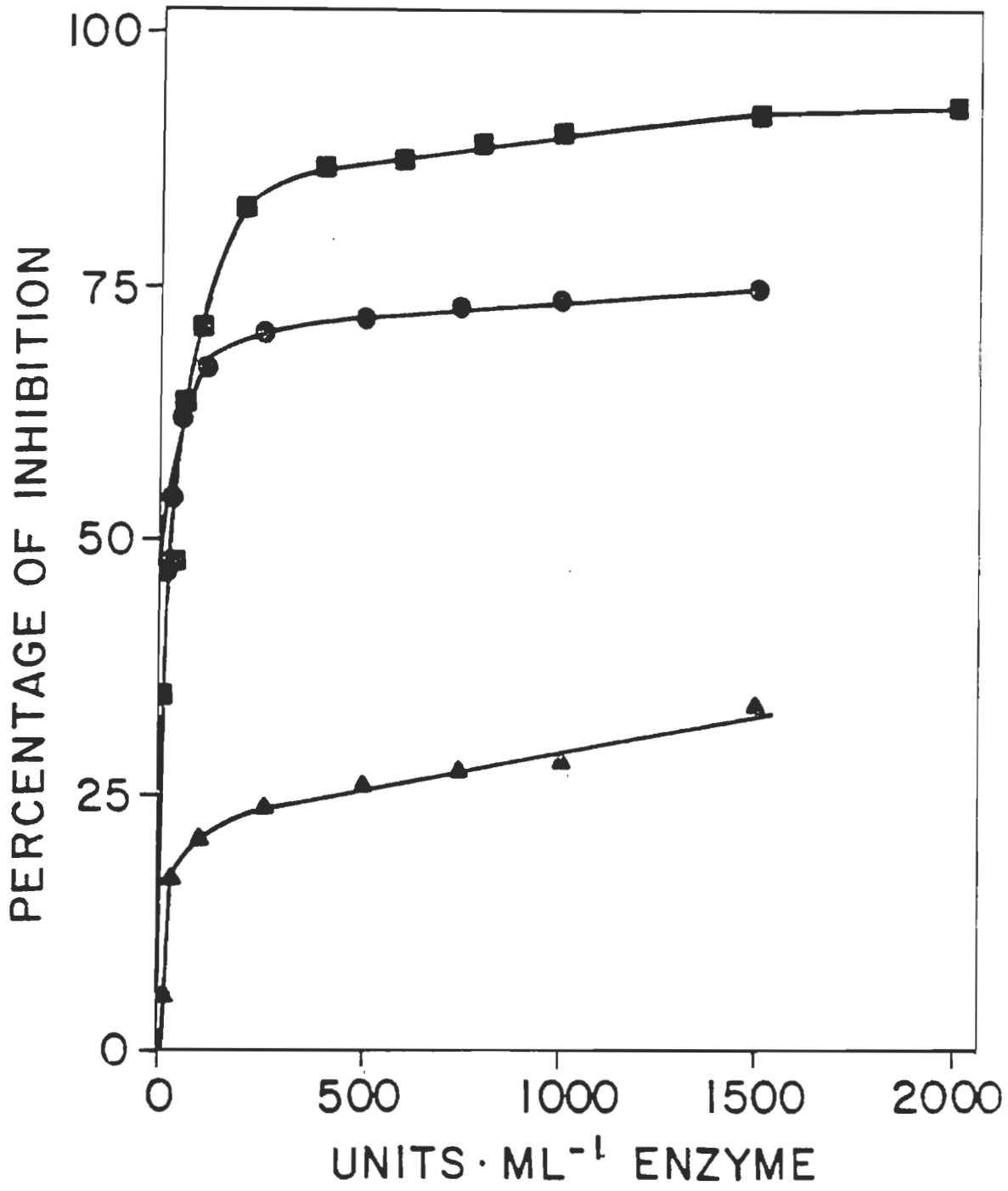

Figure 13. Inhibition of photocurrent generation by three enzymes: ▲, superoxide dismutase; ●, glucose oxidase + 4 mM glucose; ■, catalase. Initial uninhibited photocurrents averaged 5.4 μA, 4.8 μA and 4.8 μA, respectively.

superoxide dismutase could stem from the toxic effects of excess peroxide. Alternatively, another mechanism has been proposed (Allen, 1975) and is more likely responsible for the observed inhibition. It suggests that oxygen is reduced by ferredoxin in a two-step process. Reduced ferredoxin would first produce superoxide and, on being re-reduced by PS I, would have a sufficiently low redox potential to reduce superoxide to hydrogen peroxide in conjunction with two protons. The addition of superoxide dismutase would, by way of its reaction, reduce the formation rate of oxidized ferredoxin, thus inhibiting oxygen uptake (and electron transport) competitively. Such inhibition would obviously reduce the photocurrent generation in the presence of the enzyme. Unfortunately, the mechanism proved difficult to confirm unambiguously and was less than fully accepted in the literature (Halliwell, 1981). However, more recently, the mechanism was corroborated by _in vitro_ experiments with isolated ferredoxin (Hosein and Palmer, 1983). For this mechanism to be implicated in the present case would suggest a significant presence of ferredoxin associated with the thylakoid membranes. Quantitatively, this is difficult to ascertain, given the nature of the protein itself, the fact it is a weakly bond extrinsic component of thylakoids and the number of other co-enzymes involving ferredoxin as a source of reductive power. Nonetheless, even the weak inhibition clearly implicates superoxide in photocurrent production.

Lastly, if the assumption above that H_2O_2 is the electroactive species then catalase should be the best inhibitor of photocurrent. Indeed, catalase was the most potent, reaching almost 50 % inhibition with only 25 units·mL^{-1} and over 90% with 2000 units·mL^{-1}. Experiments were performed to 6000 units·mL^{-1} and more than 95 % inhibition could be achieved (data not shown). Thus, hydrogen peroxide is the end of the reductive pathway that mediates electrons between PS I in solution and the working electrode.

In order to fully characterize the amplification of the photocurrent by methyl viologen, several types of experiments were performed. The cyclic voltammogram of thylakoid membranes in the presence of methyl viologen is shown in Fig. 14. When added on its own, the extent of the photocurrent does not exceed the value found in thylakoids alone but the steady value of 22 μA is reached at a potential 130 mV lower (Fig. 14B). This shift in potential is consistant with the Nernst equation by virtue of the action of methyl viologen: it has a greater affinity to accept electrons from PS I ($k = 1.7 \times 10^8$ M^{-1}·s^{-1}; Asada and Takahashi, 1987) than does oxygen ($k \sim 10^7$ M^{-1}·s^{-1}; Asada and Nakano, 1978) and it can better reduce oxygen ($k = 7.7 \times 10^8$ M^{-1}·s^{-1}; Asada and Nakano, 1978) than can the acceptor side of the photosystem. Its virtually catalytic effect results in an increased quantity of H_2O_2 production, though not as high as in the case of superoxide dismutase (see

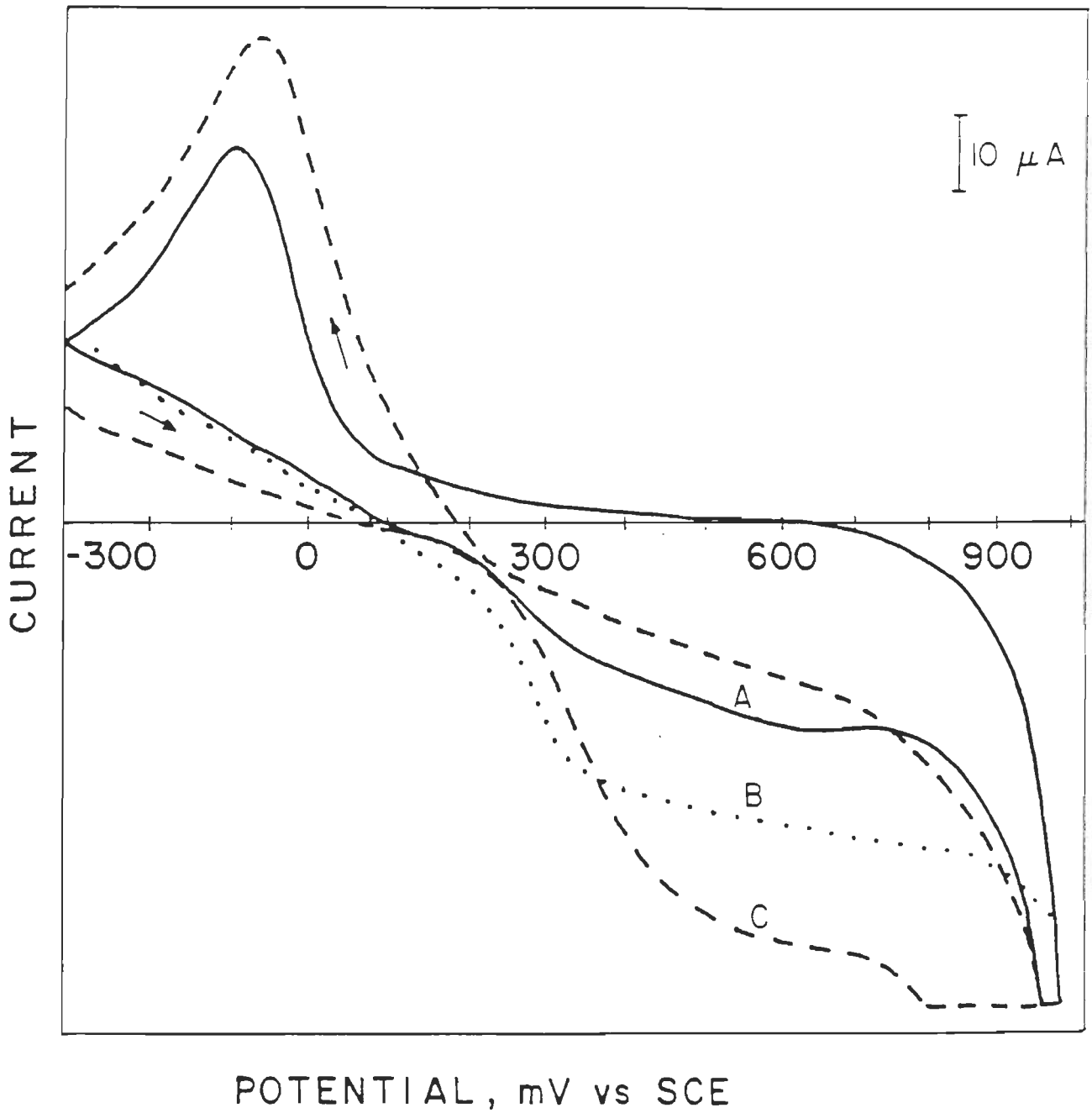

Figure 14. Cyclic voltammograms of thylakoid membranes (Chl conc. = 250 $\mu g \cdot ml^{-1}$) in the presence of 10 mM methyl viologen. A, unilluminated; B, illuminated; C, illuminated after further addition of 1 mM NH_4Cl. Scan speed = 10 $mV \cdot s^{-1}$.

kinetic rates above), that results in the shift in potential according to the equation:

$$E_{p/2} = E_o' - \frac{0.059}{2} pH + \frac{0.059}{2} \log \frac{PO_2}{[H_2O_2]}$$

(See Appendix A for derivation of this equation). If methyl viologen is used in conjunction with the uncoupling agent NH_4Cl, the photocurrent is strongly increased up to a value of 32 μA (Fig. 14C). This value is consistent with the increases observed potentiostatically and indicates the well-coupled state of the membranes. Consequently, all measurements reported in this work involving methyl viologen were performed in combination with NH_4Cl.

Figure 15 further characterizes the activation effect of methyl viologen in showing that, with increasing concentration, a sigmoidal relationship with photocurrent magnitude is remarked. Although even small concentrations of methyl viologen can increase the photocurrent significantly and large concentrations can virtually triple it, there is a range of concentration where the thylakoid membranes are particularly sensitive to the effect of the agent. The sigmoidal shape of the curve indicates that there may be a cumulative action of methyl viologen in this range. The figure also shows measurements of oxygen consumption as a function of increasing concentration of methyl viologen taken with a Clark-type electrode. The resulting curve shows a strong resemblance to that of photocurrent. Given that conditions are the same for both types of measurements (with

Figure 15. Effect of increasing methyl viologen concentration on photocurrent generation (--●--) and on oxygen uptake rates (--O--). Chlorophyll concentration was 250 $\mu g \cdot ml^{-1}$ in both cases.

I_p max , μA · mg Chl^{-1} · cm^{-2} (—●—)
O_2 UPTAKE , μmol · mg Chl^{-1} · h^{-1} (—○—)
40
30
20
10
0
0.1
1.0
10.0
1000
METHYLVIOLOGEN, μM

the notable exception of the different geometries of the oxygen uptake- and photoelectrochemical cells), the relationship gives evidence that the photoelectrochemical cell provides a comparable quantitative measure of the reduction of oxygen by thylakoid membranes.

Regardless of the magnitude of activation effects produced by thylakoids in the presence of methyl viologen, the photocurrents are also inhibited by catalase, as is shown in Fig. 16. The shape of the inhibition curve is identical to that shown in Fig. 13, with large measures of inhibition already achieved at relatively low concentrations and over 95 % inhibition at 3000 units·mL^{-1}. This demonstates that reduced methyl viologen is not an electroactive species with the working electrode and is itself not sufficient to generate photocurrents. Thus, the reduction of oxygen to H_2O_2 is obligate even in the presence of methyl viologen.

In order to characterize the inhibition by catalase, its effect on the relationship between the production of photocurrent and the chlorophyll concentration was examined in the absence and presence of catalase (at two different concentrations of catalase). Figure 17 shows that the photocurrent increases essentially linearly with chlorophyll concentration until reaching a plateau. In the presence of catalase, the enzyme clearly reduces the absolute magnitude of the photocurrent but also changes the shape of the curve; the plateau is reached more quickly (500 units·mL^{-1}

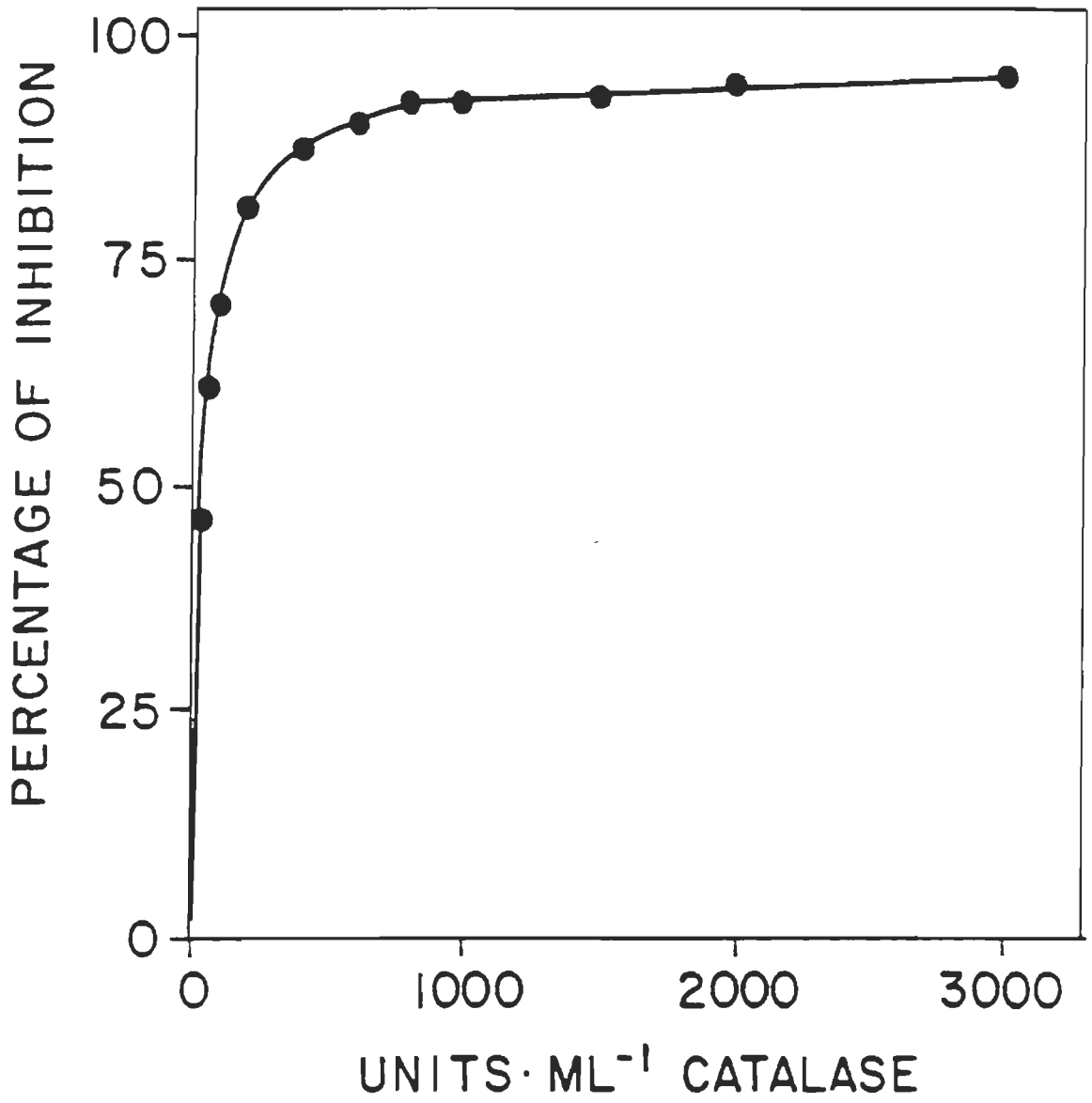

Figure 16. Inhibition by catalase of photocurrent generated by thylakoid membranes (Chl conc. = 250 $\mu g \cdot ml^{-1}$) in the presence of 1.5 μM methyl viologen. Uninhibited photocurrent was 17.4 μA.

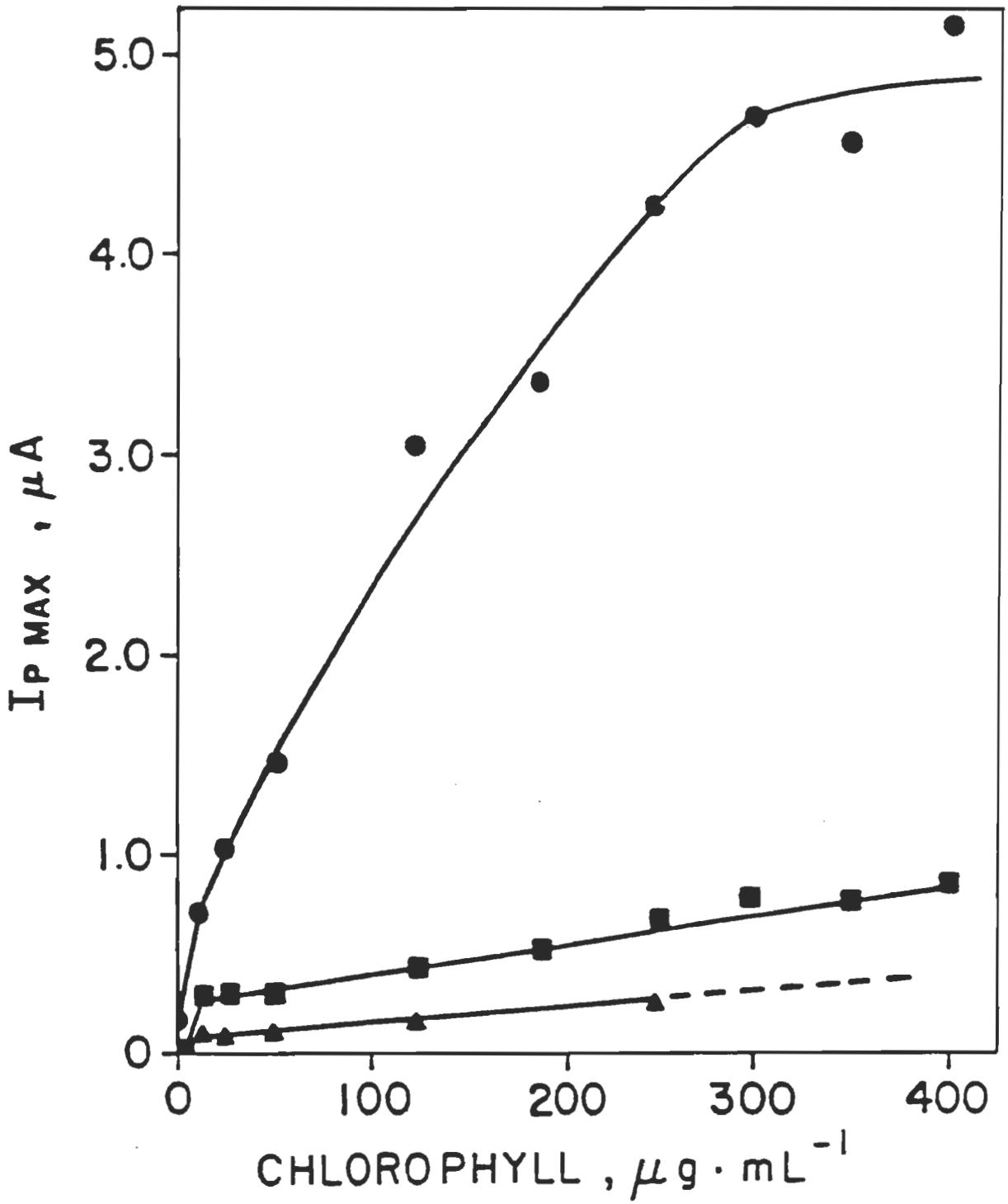

Figure 17. Relationship between the chlorophyll concentration of the thylakoid membranes and the photocurrent generated ($I_{p\ max}$), both in the presence and absence of catalase. ●, membranes alone; ■, with 500 units·mL^{-1} catalase; ▲, with 2000 units·mL^{-1}.

catalase) or immediately (2000 units·mL^{-1}). Transforming this data to a double reciprocal (Lineweaver-Burke) plot (Fig. 18), shows the lines converging on the negative side of the x-axis. This manifests catalase to exert a non-competitive type of inhibition and thus, does not interfere with the production of H_2O_2. This conclusion, though seemingly moot in the face of conclusions already drawn, shows that catalase does not inhibit photocurrent by repressing peroxide diffusion nor by restraining the thylakoids themselves in some way.

II

Up to this point, the photocurrents generated have been exclusively by thylakoid membranes containing both PS I and II. In order to better understand how they cooperatively function in thylakoids, it would be useful to separate the two and assess their indiviual functioning. Figure 19 shows the cyclic voltammogram of PS II-enriched membranes. It is quite clear that in the absence of a suitable acceptor, PS II is virtually incapable of producing photocurrent. The miniscule amount observed (Fig. 19, solid line) is most likely due to PS I contamination. This is a reasonable assumption given that the samples are not pure PS II particles but enriched membranes where PS I has been removed by detergent treatment. However, if the PS II acceptor DCBQ is added to the sample, the result is the onset of a photocurrent at approximately 50 mV and an increase of approximately 30 μA in the photocurrent at the potential

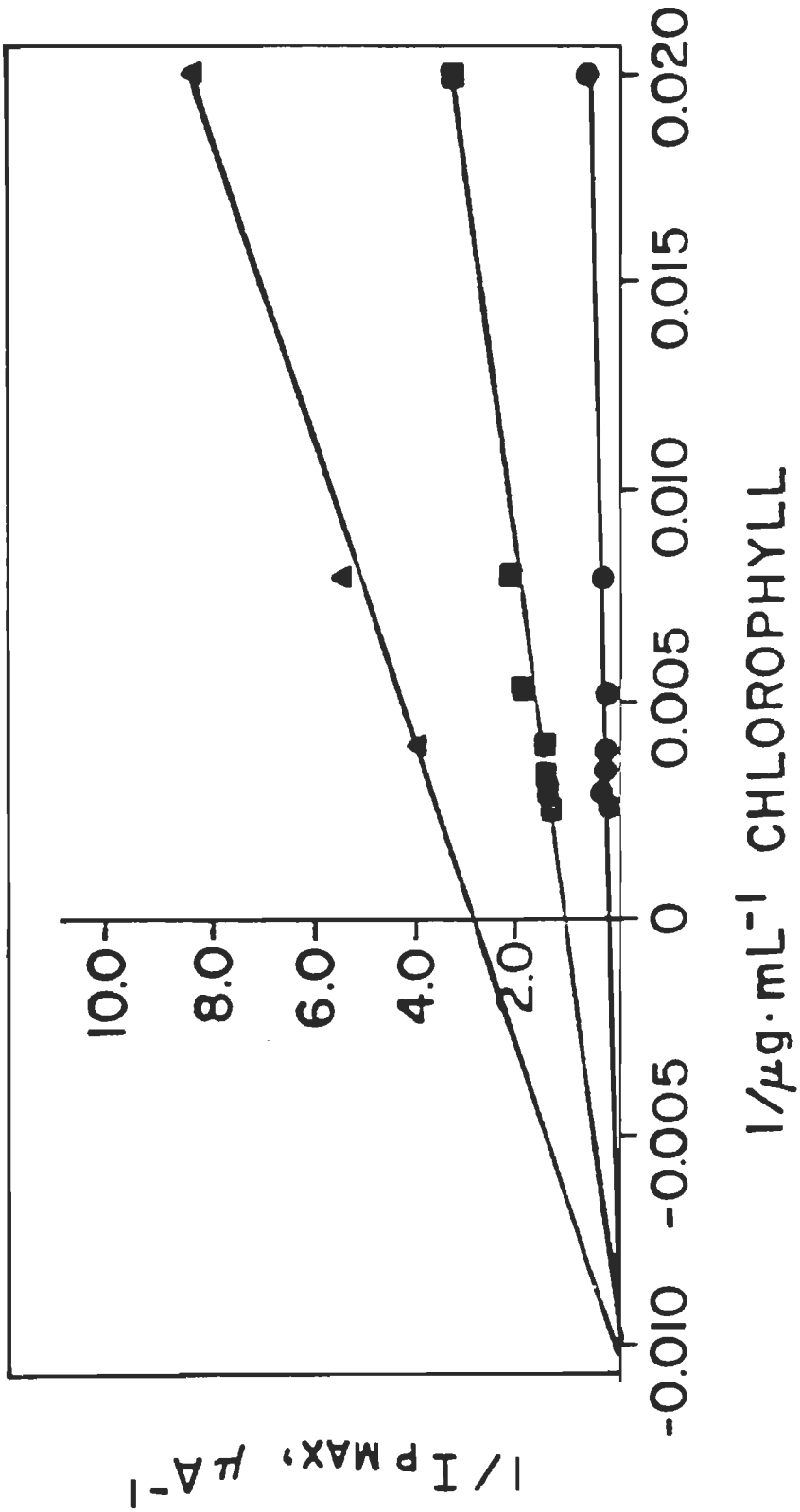

Figure 18. Double reciprocal plot of the data from Fig. 17. Lines of best fit were produced by GRAPHE v.5, run on a CYBER computer. Symbols are the same as in the preceding figure.

Figure 19. Cyclic voltammograms of PS II enriched membranes (Chl conc. = 250 $\mu g \cdot ml^{-1}$). ---, unilluminated; ——, illuminated; ···, illuminated in the presence of 0.6 mM DCBQ. Inset: cyclic voltammogram of 0.6 mM DCBQ in buffer solution. Scan speeds = 10 $mV \cdot s^{-1}$.

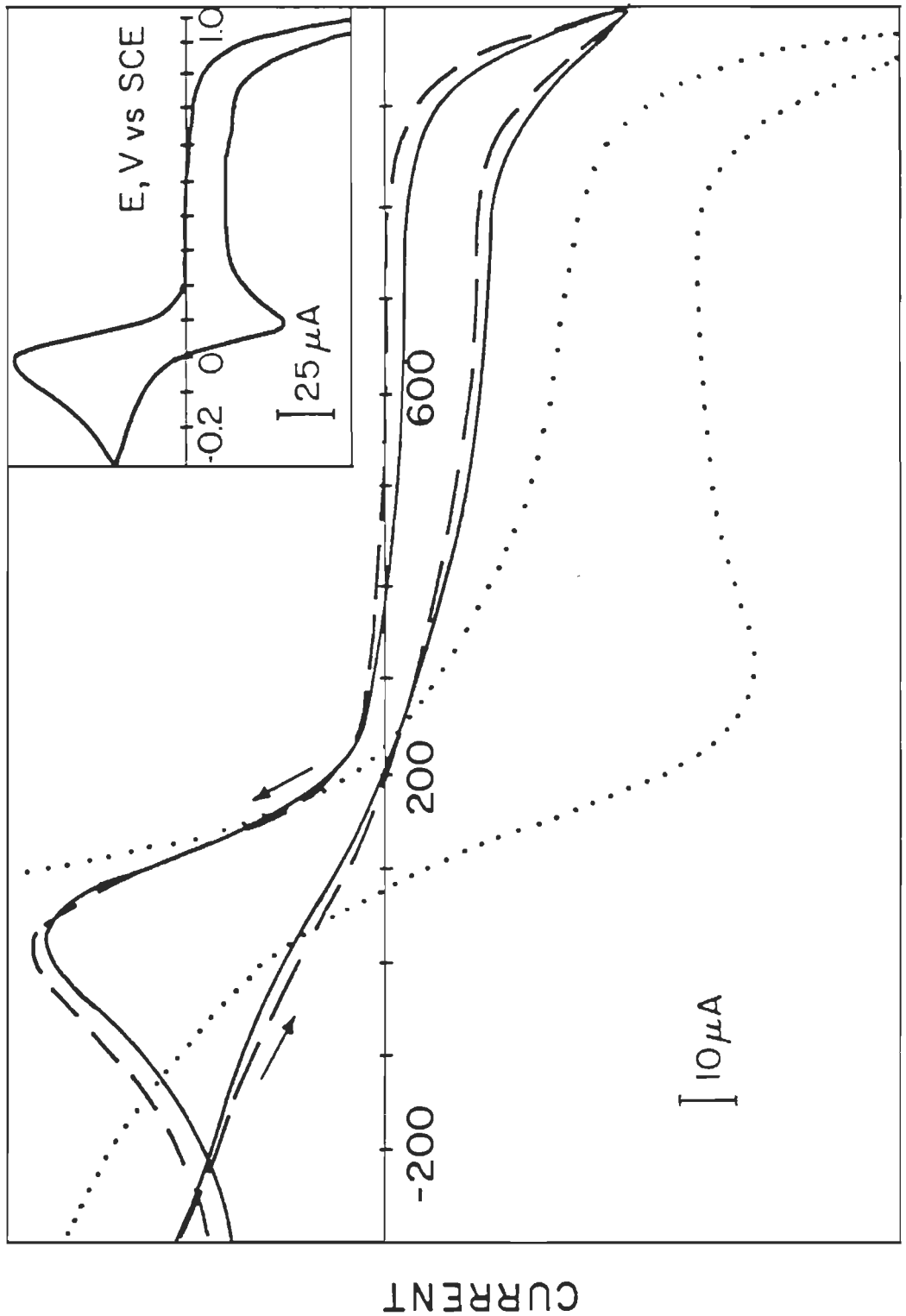
E, V vs SCE
1.0
0
-0.2
25 μA
600
200
-200
10 μA
CURRENT
POTENTIAL, mV vs SCE

corresponding to the oxidation of DCBQ, whose voltammogram in a buffer solution is reported in the inset of the same figure. No further increase in the photocurrent is recorded at higher potentials. The DCBQ peak is slightly positively shifted in the PS II voltammogram relative to the inset due to the increase in the solution resistance caused by the presence of low conducting membranes. The peak is also much broader in the PS II sample because of the "redox recycling" of the acceptor by the electrode/PS II. In other words, PS II-reduced DCBQ, once oxidized by the electrode, will be re-reduced by the photosystem. Most importantly, the combined evidence of an early photocurrent onset potential relative to thylakoids, a well defined peak rather than a plateau (also indicating a one electron process) and a negative slope of the curve in the region corresponding to H_2O_2 processes in thylakoids inexorably bar the involvement of hydrogen peroxide in the photocurrent generation. It is DCBQ that is the electroactive species in this case.

Turning to PS I enriched membranes, the samples are presumed to be incapable of producing noteworthy photocurrent in the absence of a suitable donor and thus, the cyclic voltammograms presented in Figure 20 all contain the PS I donor DQ, whose cyclic voltammogram in buffer solution is shown in the inset of the figure. This artificial agent donates electrons at the level of the plastoquinone-binding site of the cyt b_6f complex (Nanba and Katoh, 1986). In unilluminated PS I enriched membranes, two

Figure 20. Cyclic voltammograms of PS I enriched membranes (Chl conc. = 250 $\mu g \cdot ml^{-1}$). ——, unilluminated with 0.1 mM reduced DQ; ---, illuminated with 0.1 mM DQ; ···, illuminated with 0.1 mM DQ and 1.5 mM methyl viologen; -·-, as preceding with 5000 units$\cdot mL^{-1}$ catalase. Inset: cyclic voltammogram of 0.1 mM DQ in buffer solution. Scan speeds = 10 $mV \cdot s^{-1}$.

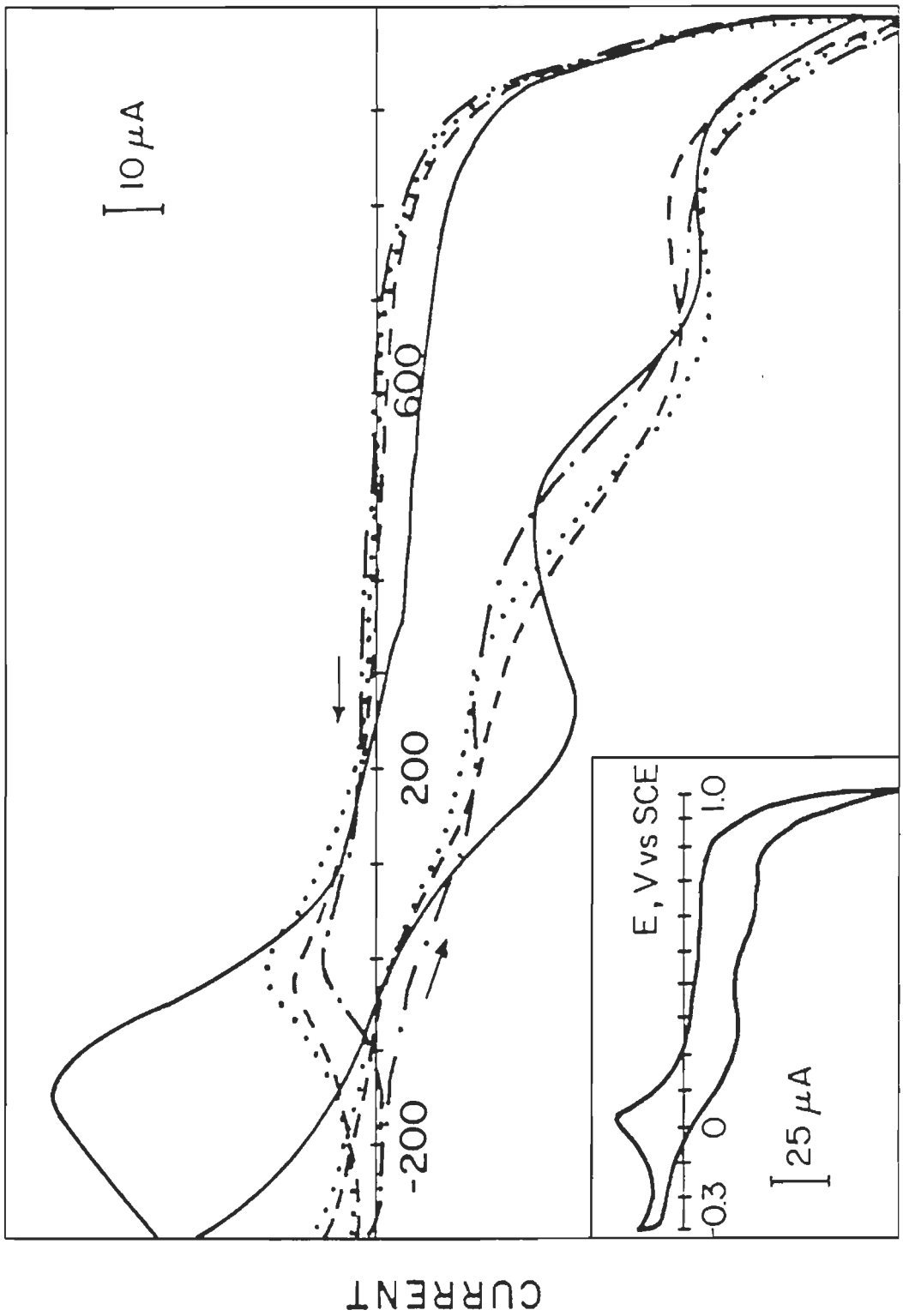
10 μA
600
200
-200
E, V vs SCE
1.0
0
-0.3
25 μA
CURRENT
POTENTIAL, mV vs SCE

oxidation peaks at approximately 250 and 700 mV, corresponding to the potentials of DQ oxidation as shown in the inset, are observed, along with a large, broad reduction peak at - 150 mV. Upon illumination, the disappearance of the lowest potential DQ oxidation peak is accompanied by a photocurrent starting at potentials somewhat lower than 300 mV and reaching a maximum of 18 μA. The addition of methyl viologen does not significantly increase the magnitude of photocurrent produced by the uncoupled membranes. Yet, even in the presence of methyl viologen, the addition of catalase results in inhibition of 85 % of the photocurrent but a maintainance of the 700 mV oxidation peak. These results show that, although DQ by itself is involved in two one-electron oxidations with the electrode, only the low potential electron is donated to PS I and commuted to photocurrent in a manner similar to thylakoids, i.e. via PS I reduction of oxygen. The high potential electron is donated to the electrode in all the displayed situations as evidenced particularly by the catalase curve. Indeed, as this electron's potential is even higher than the peroxide oxidation potential, it is not electrochemically possible for this electron to participate in photosynthetically relevant redox reactions.

Especially notable in these curves is the failure of methyl viologen to produce a large increase in photocurrent, even in uncoupled membranes. This is interpreted as proof that the electron donation by DQ is the rate limiting step

in PS I enriched membranes. However, in PS II enriched membranes, since the addition of acceptor caused a large increase in photocurrent, the electron donation step (i.e. water oxidation) cannot be rate limiting in the production of photocurrent. By corollary, in the context of thylakoid membranes, the rate limiting step is ultimately the reduction of oxygen because if the reaction rate is increased by a more efficient, faster acceptor, the reaction on the donation side (either PS I or II) seemingly does not saturate.

III

A photosynthetic action spectrum reflects the efficiency of different wavelengths of light in promoting photosynthesis. In correlating it to a corresponding absorption spectrum, the relative activities of pigments can be established. For these reasons, the action and absorption spectra were measured for thylakoid membranes and PS I- and PS II enriched membranes. From these results, while not definitively quantitative, there emerge a number of noteworthy points.

The spectra of thylakoid membranes are shown in Figure 21. The absorption spectrum is characterized by bands for Chl a (681 and 440 nm), Chl b (653 and 475 nm), their associated minor bands (622 and 584 nm) and a carotenoid peak at 486 nm. The spectrum is consistent with classic spectra in the literature (see Lehninger, 1982, p. 655, for

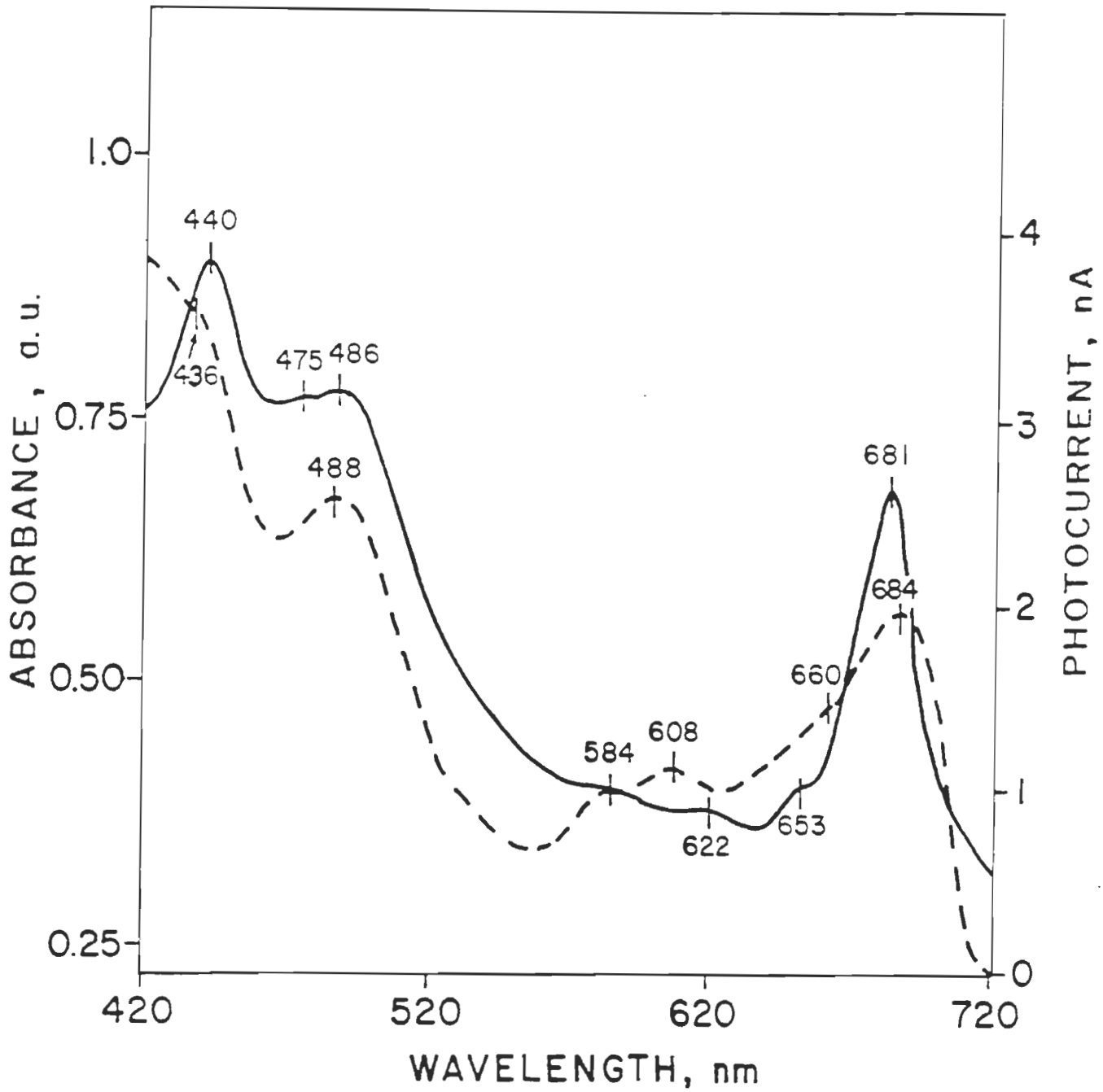

Figure 21. Action (---) and absorption (——) spectra of thylakoid membranes (Chl conc. = 10 $\mu g \cdot ml^{-1}$). Action spectra were obtained under potentiostatic conditions of -140 mV vs. SCE (100 mV vs. SHE).

quick reference). In comparison, the action spectrum of thylakoids in the photoelectrochemical cell is not only similar in shape to the absorption spectrum but evidences most of the same peaks (the exception being 475 nm), though they now show slight red shifts. It should be noted that the sharply increasing photocurrent at the shortest wavelengths is considered to be an artifact, perhaps related to the photoeffect of platinum mentioned earlier. This is a reasonable inference because of the relatively high energy of these wavelengths and magnitude of photocurrent generated. The consistency of form and position of the action spectrum indicates that the strongly absorbing pigments of thylakoids are also ultimately involved in the reduction of oxygen. The cooperative functioning of PS I and II is displayed in the broadness of the long wavelength Chl a action peak relative to its absorption, not only in its red shift but also in the vague, poorly defined shoulder at approximately 700 nm. Further remarkable, is the rather large contribution of carotenoids to the photocurrent, reflecting that these pigments have well coupled energy transfer to the reaction centers. This is consistent with their secondary role of broadening the available spectral energy range for photosynthetic organisms (Cogdell, 1988).

In PS II enriched membranes (Fig. 22), the action spectrum also corresponds well to the absorption counterpart. Essentially the same peaks are produced as in the case of thylakoids but the long wavelength Chl a peak is

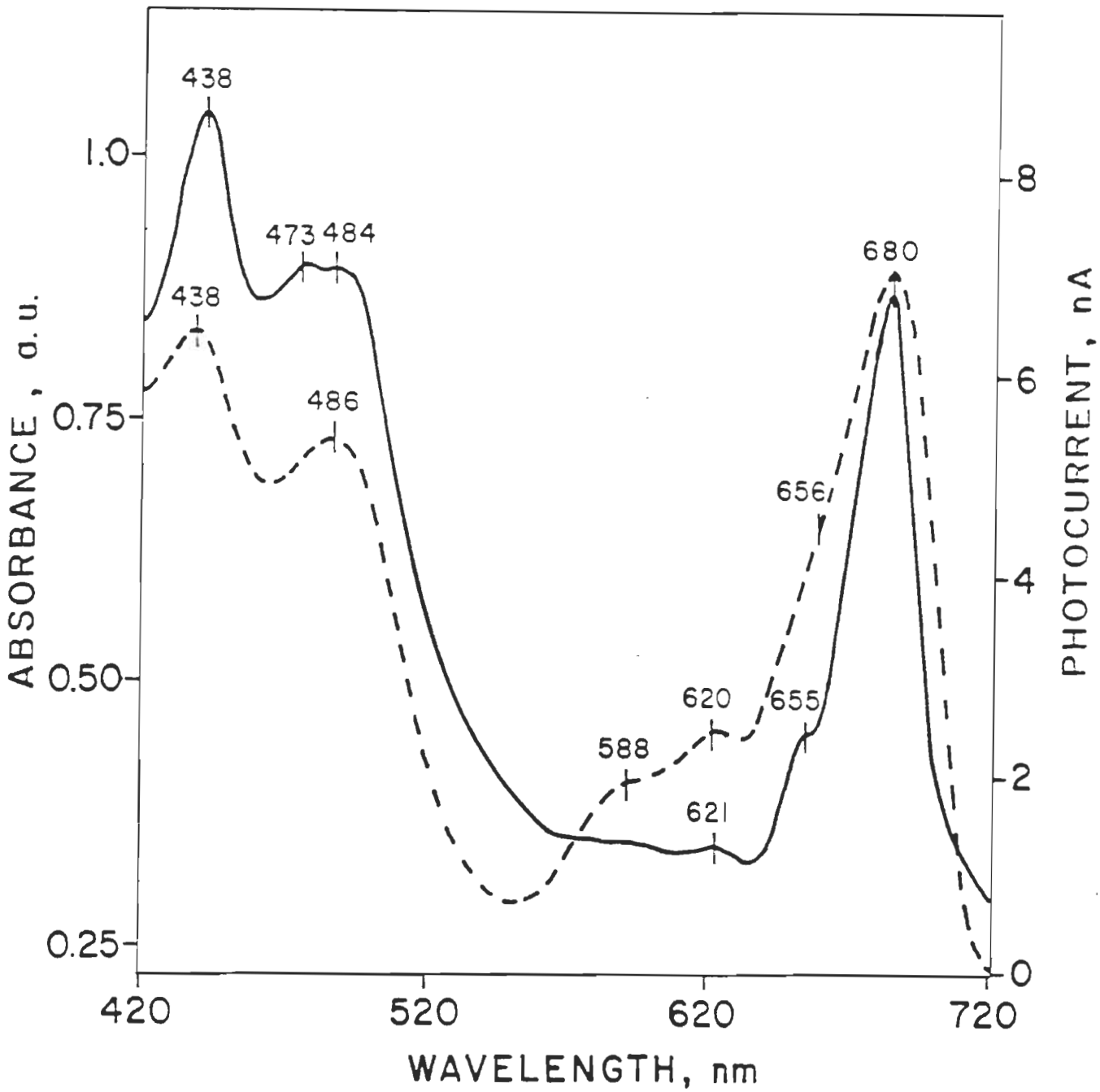

Figure 22. Action (---) and absorption (——) spectra of PS II enriched membranes (Chl conc. = 10 $\mu g \cdot ml^{-1}$). Action spectra were obtained in the presence of 0.2 mM DCBQ under potentiostatic conditions of -140 mV vs. SCE (100 mV vs. SHE).

narrower, more in proportion with the absorption band, and the general red shift effect is less pronounced, mirroring the more direct production of photocurrent by the PS II/DCBQ system. Moreover, the carotenoids again play a significant role in energy transfer, as in thylakoids.

However, PS I enriched membranes exhibit quite different behavior than PS II. In this case, the absorption spectrum (Fig. 23) is void of indentifiable Chl b bands and shows only Chl a peaks (680 and 438 nm, with minor peaks at 624 and 592 nm) and that of carotenoids at 470 nm (though the magnitude of the 438 nm band skews this peak and makes identifying its exact maximum difficult). This absence is consistent with the increased Chl a:b ratios of PS I given in the literature (Melis, 1989). The action spectrum is invariant in this attribute but reveals a PS I-unique splitting of the long wavelength Chl a action peak (696 and 670 nm). This seemingly shows a reaction center photocurrent generation efficiency comparable to PS II but also evinces a separate antennae Chl a component. Since the antennae itself cannot be directly involved in oxygen (or methyl viologen, for that matter) reduction, its distinct peak would confirm its increased light harvesting capacity relative to PS II antennae (Melis, 1989) and further, a very strongly coupled energy transfer to the reaction center. Furthermore, the relatively small photocurrent contribution of carotenoids observed in PS I, as measured by the relative peak heights of the carotenoid vs long wavelength Chl a

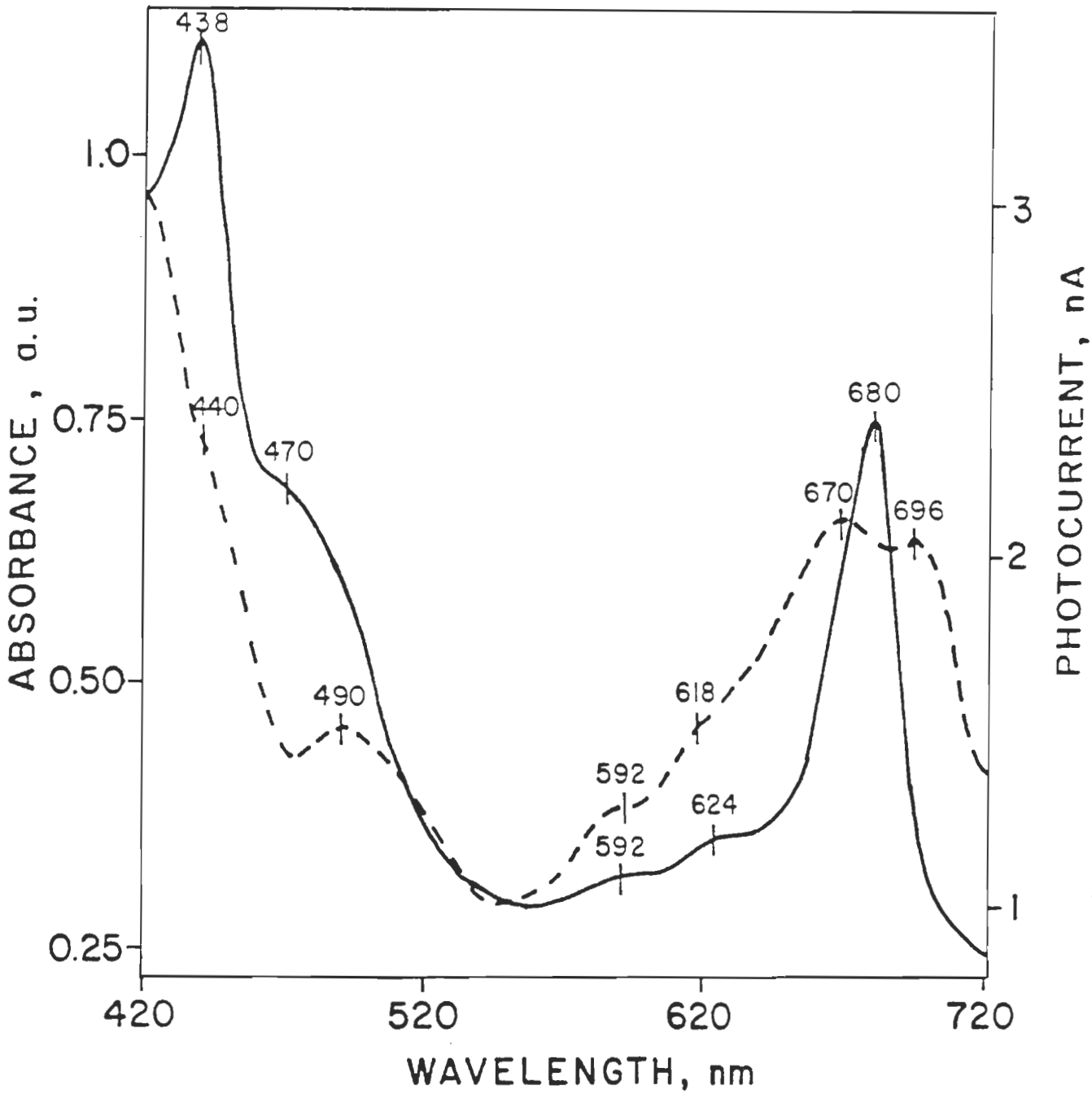

Figure 23. Action (---) and absorption (——) spectra of PS I enriched membranes (Chl conc. = 10 $\mu g \cdot ml^{-1}$). Action spectra were obtained in the presence of 0.5 mM reduced duroquinone and 0.5 mM methyl viologen under potentiostatic conditions of 0 mV vs. SCE (240 mV vs. SHE).

peaks in the three membrane preparations, is equable with the larger set of carotenoids in PS II and associated antennae than in the PS I system (Goodwin and Britton, 1988).

Considered collectively, the action spectra have shown that, in the photoelectrochemical cell, the major photosynthetic pigment components of the membrane preparations are intact and functioning in a cooperative, coupled manner, such as would be expected *in vivo* or at least, in other comparable *in vitro* systems. Thus, the usefulness of the photoelectrochemical cell as a tool for studying photosynthesis may extend to investigating agents or circumstances that affect the intramembrane (or intra-photosystem) energy transfer events.

IV

As a mechanistic model, the photoelectrochemical cell monitors the activity of PS I while in thylakoid membranes, where PS II is the donor and ambient dissolved oxygen (or methyl viologen) is the acceptor. Electrons are mediated to the working electrode via a Mehler reaction pathway. This opens up the possibility of monitoring pseudocyclic electron transport more directly than has previously been possible. As mentioned in the Introduction, this process is usually detected by mass spectrometer or Clark electrode experiments measuring oxygen uptake in illuminated chloroplasts. However, such measurements are complicated by the uptake of

oxygen by other metabolic pathways. The contribution of glycollate synthesis can be effectively eliminated Egneus et al, 1975) but the oxygen consumption by metabolism of phenolic compounds remains a problem (Halliwell, 1981). The photoelectrochemical cell overcomes these types of difficulties by directly monitoring the reduction of oxygen in thylakoid (or enriched) membranes. This system, by its nature, allows oxygen to compete more proficiently for electrons because, owing to the isolation procedures, the membranes have lost the inherent enzymes that protect chloroplasts *in vivo* from the otherwise toxic products of the Mehler reaction. Thus, the pathway proceeds largely unhindered.

The data demonstrate the potential application for manipulating the reducing side of PS I and further investigating both the role of the pseudocyclic electron transfer pathway and such endogenous post-PS I acceptors such as ferredoxin and FNR. In fact, a preparation of spinach ferredoxin was commercially obtained and the effect of its concentration on the photocurrent generated by thylakoid membranes in shown in Fig. 24. Its activity is marked by a gradual increase of photocurrent until a plateau is achieved at 60 μM concentration. It produced a maximal increase of 40 % over control thylakoids and had an I_{50} = 16.2 μM. Curiously, when ferredoxin was biochemically prepared according to the method of Yocum et al (1975), the isolate caused a decrease in photocurrent, as also shown in

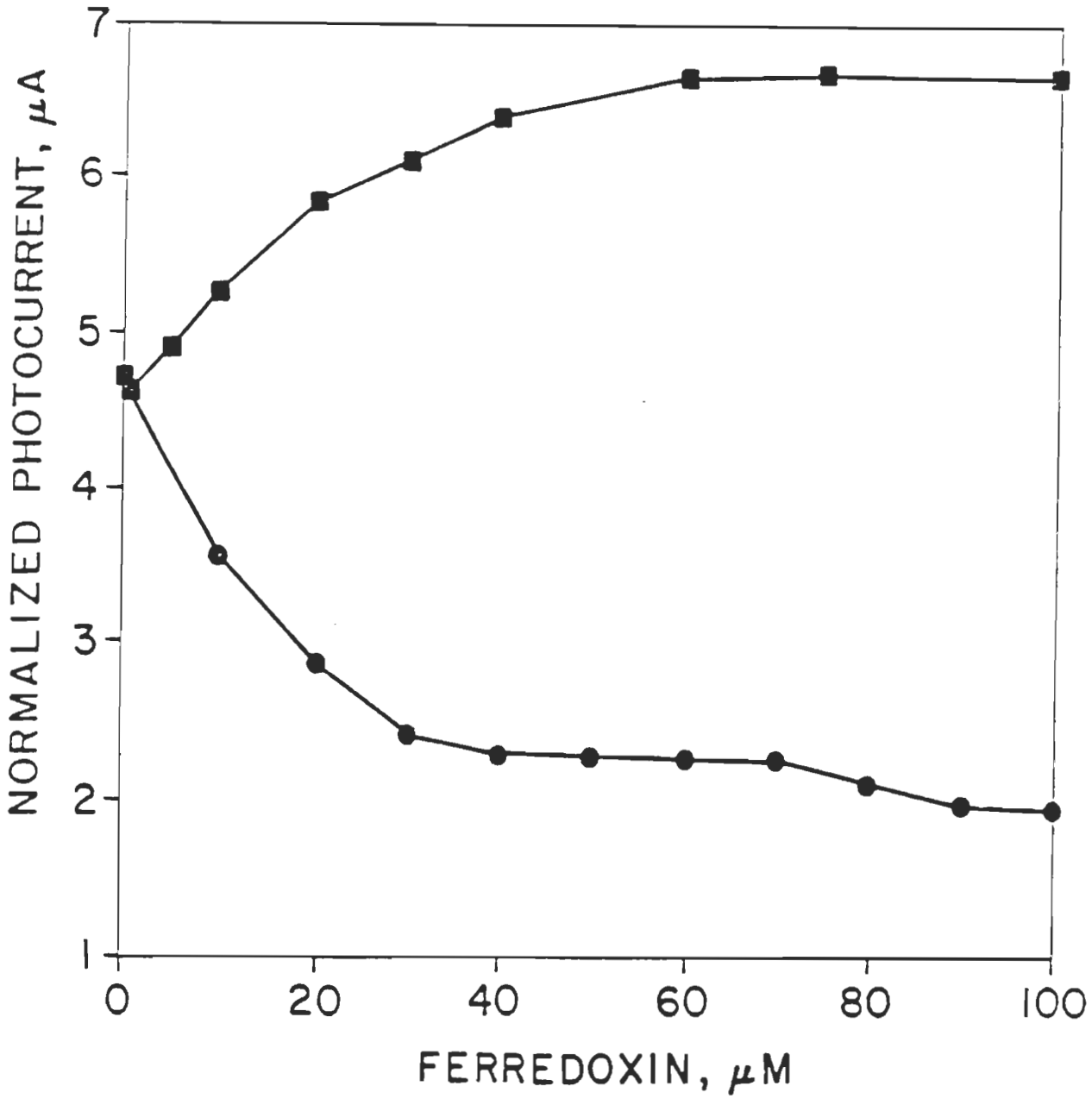

Figure 24. Effect of isolated pure ferredoxin (-●-) and commercially obtained ferredoxin (-■-) on photocurrent generation of thylakoid membranes (Chl conc. = 250 $\mu g \cdot ml^{-1}$). Photocurrents were normalized to 4.7 μA control photocurrent.

Fig. 24. The shape of the curve produced, its plateau attained at 50 μM, was remarkably similar to that of the commercial product and I_{50} = 11.5 μM. Its maximaum inhibition was 59 % of control. Further, the isolate's absorption spectrum and its A_{420}/A_{276} ratio were consistent with the literature, identifying it as pure oxidized ferredoxin. Yet ferredoxin is known to form a strong, electrostatically bound complex with FNR (see above), so an electrophoresis gel was used to analyze the constituents of each ferredoxin. Figure 25 shows the densitometer scan of the resulting Coomassie stained gel and clearly shows the biochemically isolated ferredoxin to have but one absorption band (Fig. 25B), evincing its purity. The commercial product, however, displays two absorption bands (Fig. 25A). The band of farthest migration is most certainly equivalent to the single band on the lower scan and, therefore, ferredoxin and the other band corresponds to the molecular weight of FNR, based on its migration distance. However, neither of the proteins migrated to the exact positions appropriate to their molecular weight; ferredoxin because it possesses an overall negative charge (Scheller et al, 1988; Andersen et al, 1990) due to amino acid composition that somewhat impedes its migration and FNR, in this case, because of the presence of a high quantity of NaCl (0.5 M) necessary to cleave the complex with ferredoxin (Zanetti and Curti, 1981). Molecular standards are not displayed for

Figure 25. Densitommeter scans of SDS-polyacrylamide (10-15 % gradient) electrophoresis gels of the commercially obtained ferredoxin (A) and the isolated pure ferredoxin (B). Smallest polypeptides have the farthest migration distance.

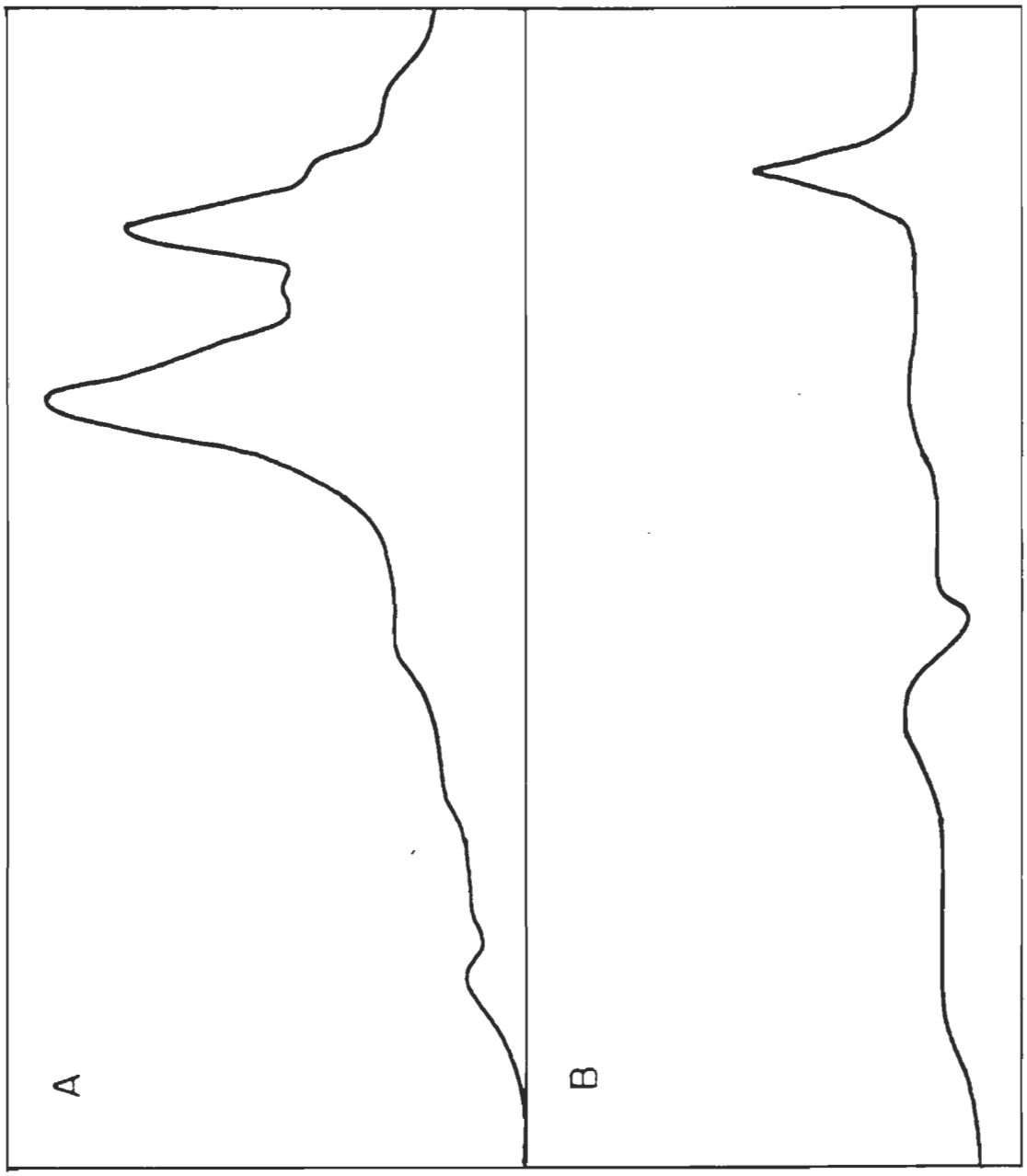
A
B
ABSORBANCE , rel. units
MIGRATION DIRECTION

these reasons. However, further evidence of the identification of FNR is provided immediately below.

Table 2 summarizes the results of two series of experiments performed using the commercially obtained ferredoxin in conjunction with catalase and $NADP^+$. The results show that the physiological acceptor constitutes a formidable inhibitor of the photocurrent, even accentuating the inhibition of catalase. Since the activity of FNR is specific for $NADP^+$ (Forti et al, 1983; Karplus et al, 1984), this acceptor would be expected to be preferentially reduced over oxygen, if it is available. That it is able to inhibit photocurrent to the same extent whether or not catalase is present, suggests that oxygen competes with the physiological acceptor for PS I electrons. Direct evidence of this relationship is difficult to gather because of the nature of the acceptors: dissolved oxygen concentration is difficult to control and the quantity of $NADP^+$ reduced would be dependent on individual thylakoid preparation activity, which varies for ovious reasons. Nonetheless, the direct competition between the two at the same site is a defensible presumption, given the $NADP^+$ inhibition data and that the presence of FNR produces a catalase-sensitive increase in photocurrent, as shown in Figure 24 and Table 2B. As further indirect proof, X-ray crystallography data of the structure of FNR showed only two active sites for the enzyme, at the carboxy-terminal end (for $NADP^+$) and the amino-terminal end for interaction with ferredoxin (Karplus et al, 1984).

Table 2. Effect of $NADP^+$ on photocurrent under different conditions.

	CONDITIONS	PHOTOCURRENT (μA)
A	Control	5.4
	+ 50 μM Ferredoxin	6.5
	+ 50 μM Ferredoxin and 100 μM $NADP^+$	0.2
B	Control	5.0
	+ 4000 units·mL^{-1} Catalase	0.8
	+ 4000 units·mL^{-1} Catalase and 50 μM Ferredoxin	1.3
	+ 4000 units·mL^{-1} catalase, 50 μM Ferredoxin and 100 μM $NADP^+$	0.1

Data obtained using thylakoid membranes having a Chl concentration of 250 $\mu g \cdot mL^{-1}$ under 750 mV imposed potential.

Furthermore, although it has been shown in *in vitro* experiments involving artificially reduced isolated ferredoxin on its own, that ferredoxin can indeed univalently reduce oxygen (Hosein and Palmer, 1983), the results in Fig. 24 suggest that ferredoxin added to the thylakoids did not possess this ability. This might have been due to the ferredoxin not becoming involved with the membranes at all but this is inconsistent with the inhibition produced. Moreover, its absorption spectra indicated that, not only was the isolated ferredoxin oxidized, but that its Fe-S center was intact and therefore, able to be reduced by PS I.

Overall, the data strongly implicate FNR providing the site of oxygen reduction in the thylakoid membranes in the photoelectrochemical cell. By extension to an *in vivo* context, the pseudocyclic electron transfer pathway competes directly with $NADP^+$ reduction, as is summarized in Fig. 26. If so, this would have a number of advantageous metabolic consequences for chloroplast physiology. Firstly, the pseudocyclic electron transport pathway would represent a true attenuating mechanism for the redox state of the $NADP^+$/NADPH pool. Invoking it would, as already mentioned, not only abate the formation of NADPH but also consume it due to the scavenging apparatus of chloroplasts (Figs. 26 and 4). Relatedly, this pathway could be used to raise the ratio of ATP/NADPH produced during the course of electron transport if metabolic demands required more ATP, i.e. to

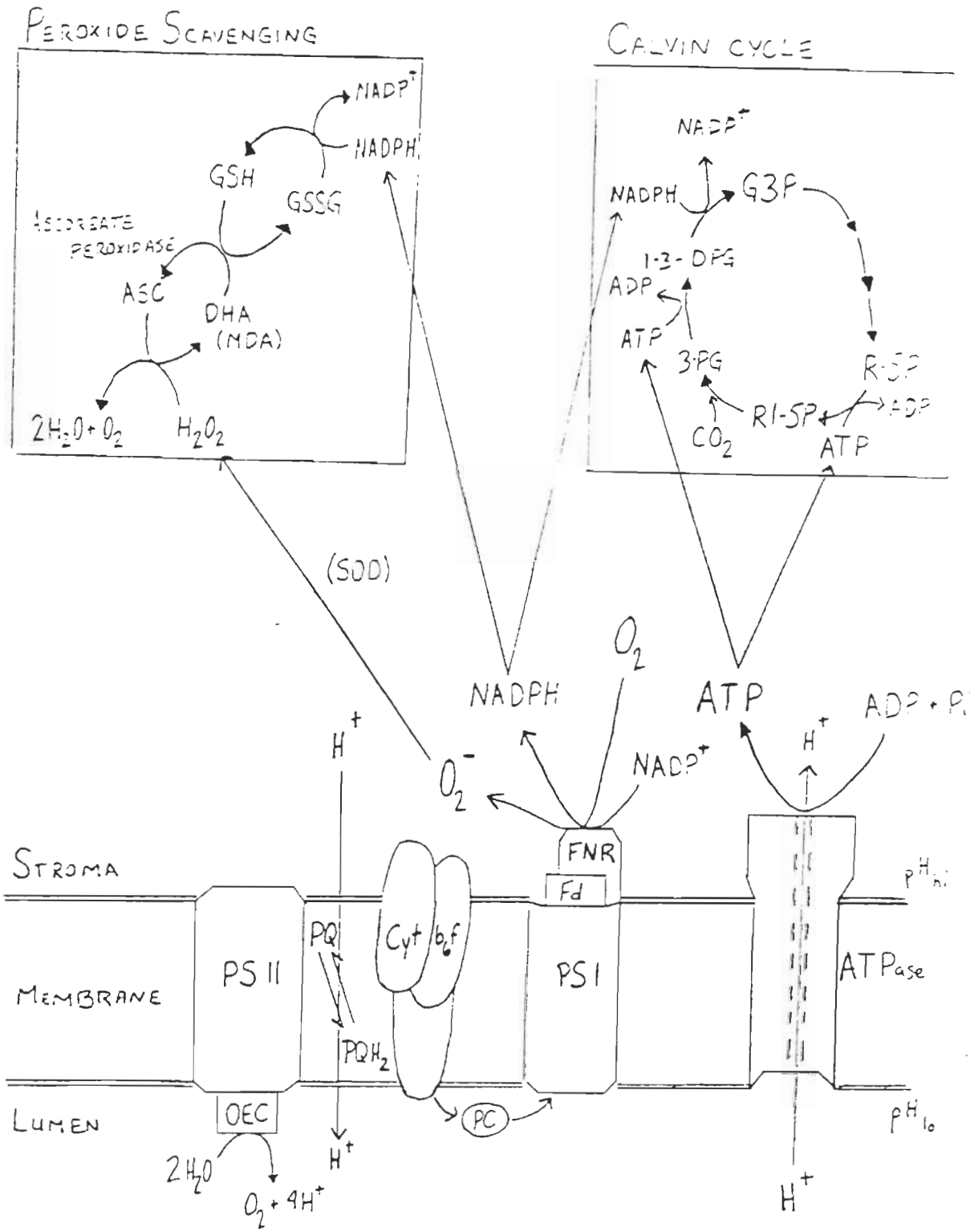

Figure 26. Summary of the implications of the proposed reduction site of oxygen as FNR. The model suggests immediate attenuation of NADPH formation and its consumption by peroxide scanvenging during pseudocyclic electron transport.

enhance carbon dioxide assimilation. Secondly, as such, it would also constitute an excellent coping mechanism in the case of elevated electron transport rates, i.e. during conditions of high photon flux densities. Lastly, it is undoubtedly a faster response to any of the above stresses or demands than cyclic electron transport would be, simply based on the obligate diffusion component inherent in the latter pathway. This, of course, does not in any way rule out the occurrence of the cyclic pathway (nor would the data support such conjecture) but it is consistent with the conclusion of Steiger and Beck (1981) that the cyclic pathway does not inhere an alternative to the pseudocyclic pathway but is, in fact, dependent on it.

CONCLUSIONS

The results of this study of a unichambered photoelectrochemical cell lead to the following conclusions:

- the observed photocurrent is generated by PS I-reduced oxygen, mediated to the working electrode by a Mehler reaction type pathway, analogous to the pseudocyclic electron transport pathway observed in plant cells. The photoelectrochemical cell thus constitutes an excellent tool for studying the reducing side of PS I.
- the photoelectrochemical cell has been shown to be directly comparable to conventional techniques of measuring photosynthetic oxygen reduction. Further, the photocurrent can be both amplified and inhibited by exogenously added agents.
- the reducing site of FNR has been suggested to be the site of oxygen reduction by PS I. Given the elaborate *in vivo* scavenging mechanism of hydrogen peroxide, the site has distinct advantages in terms of the plant cell's ability to balance its NADP/ATP requirements.

APPENDIX A

To calculate the half-peak potential shift caused by the increased production of hydrogen peroxide due to the addition of methyl viologen, the Nernst equation is used:

$$E_{p/2} = E_o' + \frac{2.303\ R\ T}{n\ F} \log Q$$

where $E_{p/2}$ = observed half-peak potential,

E_o' = standard potential for the reaction at STP,

R = gas constant 1.987 $cal \cdot mol^{-1} \cdot K^{-1}$,

T = absolute temperature 297 K,

n = number of electrons involved in half reaction,

F = Faraday's constant 23 060 $cal \cdot V^{-1} \cdot (mol\ e^-)^{-1}$,

Q = reaction quotient [oxidized]/[reduced] species

Expressed with the constants calculated in:

$$E_{p/2} = E_o' + \frac{0.0592}{n} \log \frac{[oxi]}{[red]}$$

Given the reaction for the degradation of hydrogen peroxide at a platinum electrode:

$$2\ H_2O_2 \rightarrow 2\ H_2O + O_2,$$

the half reactions are:

$$H_2O_2 + 2H^+ + 2e^- \rightarrow 2H_2O \quad (red.\ eq^n)$$

$$H_2O_2 \rightarrow O_2 + 2H^+ + 2e^- \quad (oxi.\ eq^n)$$

and substituting into the Nernst equation:

$$E_{p/2} = E_o' + \frac{0.0592}{2} \log \frac{[H^+]\ PO_2}{[H_2O_2]}$$

where PO_2 = partial pressure of O_2. Separating the terms gives:

$$E_{p/2} = E_o' + \frac{0.0592}{2} \log [H^+] + \frac{0.0592}{2} \log \frac{PO_2}{[H_2O_2]}$$

Lastly, since $- \log [H^+] = pH$, then:

$$E_{p/2} = E_o' - \frac{0.0592}{2} pH + \frac{0.0592}{2} \log \frac{PO_2}{[H_2O_2]}$$

REFERENCES

Adam, Z. and R. Malkin (1987) Reconstitution of isolated Rieske Fe-S protein into a Rieske-depleted cytochrome b_6-f complex. FEBS Lett. **225**, 67-71.

Agostiano, A., A. Ceglie and D. Della Monica (1984) Water photoelectrolysis through the use of electrodes covered by photosystems I and II. Bioelectrochem. Bioenerg. **12**, 499-511.

Agostiano, A. and F. K. Fong (1987) In vitro photoelectrochemical model of the Z scheme in green plant photosynthesis. Bioelectrochem. Bioenerg. **17**, 325-337.

Agostiano, A., D. C. Goetze and R. Carpentier (1990) Cyclic voltammetry measurements of the photoelectrogenic reactions of thylakoid membranes. In submission to Photochem. Photobiol.

Alberts, B, D. Bray, J. Lewis, M. Raff, K. Roberts and J. D. Watson (1983) Molecular biology of the cell. Garland Publishing, Inc., New York. p. 512.

Allen, J. F. (1975) A two **step** mechanism for the photosynthetic reduction of oxygen by ferredoxin. Biochem. Biophys. Res. Comm. **66**, 36-43.

Allen, M. J. and A. E. Crane (1976) Null potential voltammetry - an approach to the study of plant photosystems. Bioelectrochem. Bioenerg. **3**, 84-91.

Andersen, B., B. Koch, H. V. Scheller, J. S. Okkels and B. L. Moller (1990) Nearest neighbour analysis of the photosystem I subunits in barley and their binding of ferredoxin. In: Current Research in Photosynthesis (Ed. M. Baltscheffsky), Vol. 2. Kluwer Academic Publishers, Dordrecht. pp. 671-674.

Anderson, J. M. and A. Melis (1983) Localization of different photosystems in separate regions of chloroplast membranes. Proc. Nat. Acad. Sci. USA **80**, 745-749.

Andersson, B. and J. M. Anderson (1980) Lateral heterogeneity in the distribution of chlorophyll-protein complexes of the thylakoid membranes of spinach chloroplasts. Biochim. Biophys. Acta **593**, 427-440.

Andersson, B. and W. Haehnel (1982) Location of photosystem I and photosystem II reaction centers in different thylakoid regions of stacked chloroplasts. FEBS Lett. **146**, 13-17.

Andréasson, L.-E. and T. Vänngård (1988) Electron transport in photosystems I and II. Ann. Rev. Plant Physiol. **39**, 379-411.

Arnon, D. I. (1949) Copper enzymes in isolated chloroplasts. Polyphenyloxidase in Beta vulgaris. Plant Physiol. **24**, 1-15.

Arnon, D. I., H. Y. Tsujimoto and B. D. McSwain (1964) Proc. Natl. Acad. Sci. USA **51**, 1274-1282.

Arnon, D. I. and R. K. Chain (1975) Regulation of ferredoxin-catalyzed photosynthetic phosphorylations. Proc. Natl. Acad. Sci. USA **72**, 4961-4965.

Asada, K. and Y. Nakano (1978) Affinity for oxygen in photoreduction of molecular oxygen and scanvenging of hydrogen peroxide in spinach chloroplasts. Photochem. Photobiol. **28**, 917-920.

Asada, K. and M. Takahashi (1987) Production and scavenging of active oxygen in photosynthesis. In: Photoinhibition (D. Kyle, C. Osmond and C. J. Arntzen, eds.), Elsevier, Amsterdam. pp. 227-287.

Babcock, G. T., B. A. Barry, R. J Debus, C. W. Higanson, M. Atamian, L. McIntosh, I. Sithole and C. F. Yocum (1989) Water oxidation in photosystem II: from radical chemistry to multielectron chemistry. Biochemistry **28**, 9557-9565.

Barber, J. (1990) Electron transfer processes within the isolated reaction center of photosystem two. Invited talk, C5 Symposium: Control of Charge Transfer in Cytochrome and Chlorophyll Complexes, Concordia Univer., Montréal, August 1990.

Bard, A. J and L. R. Faulkner (1980) Elecrochemical methods. Wiley and Sons, New York. pp. 445 and 700.

Barry, B. A. and G. T. Babcock (1987) Characterization of the tyrosine radical involved in photosynthetic oxygen evolution. Proc. Natl. Acad. Sci. USA **84**, 7099-7103.

Berthold, D. A., G. T. Babcock and C. F. Yocum (1981) A highly resolved oxygen-evolving photosystem II preparation from spinach thylakoid membranes. FEBS Lett. **134**, 231-234.

Bhardwaj, R., R. L. Pan and E. L. Gross (1981) Solar energy conversion by chloroplast photoelectrochemical cells. Nature **298**, 396-398.

Biggins, J., N. A. Tanguay and H. A. Frank (1989) Electron transfer reactions in photosystem I following vitamin K_1 depletion by ultraviolet irradiation. FEBS Lett. **250**, 271-274.

Böhme, H. (1977) On the role of ferredoxin and ferredoxin-$NADP^+$ oxioreductase in cyclic electron transport of spinach chloroplasts. Eur. J. Biochem. **72**, 283-289.

Brettel, K., P. Sétif and P. Mathis (1986) Flash-induced absorption changes in photosystem I at low temperature: evidence that the electron acceptor A_1 is vitamin K_1. FEBS Lett. **203**, 220-224.

Buchanan, B. B. and D. I. Arnon (1971) Ferredoxin from photosynthetic bacteria, algae and higher plants. Meth. Enzymol. **23**, 413-440.

Chitnis, P. R., P. A. Reilly and N. Nelson (1989) Insertional inactivation of the gene encoding subunit II of photosystem I from the cyanobacterium Synechocystis sp. PCC 6803. J. Biol. Chem. **264**, 18381-18385

Clark, R. D., M. J. Hawkesford, S. J. Coughlan, J. Bennett and G. Hind (1984) Association of ferredoxin-$NADP^+$ oxioreductase with the chloroplast cytochrome b-f complex. FEBS Lett. **174**, 137-142.

Cogdell, R. (1988) The function of pigment in chloroplasts. In: Plant Pigments (T. W. Goodwin, ed.), Academic Press, London. pp. 183-230.

Crofts, A. R. and C. A. Wraight (1983) The electrochemical domain of photosynthesis. Biochim. Biophys. Acta **726**, 149-185.

Doyle, M. P., L.-B. Li, L. Yu and C.-A. Yu (1989) Identification of a M_r = 17 000 protein as the plastoquinone-binding protein in the cytochrome b_6-f complex from spinach chloroplasts. J. Biol. Chem. **264**, 1387-1392.

Droppa, M. and G. Horváth (1990) The role of copper in photosynthesis. Crit. Rev. Plant Sci. **9**, 111-123.

Egneus, H., U. Heber, U. Matthiesen and M. Kirk (1975) Reduction of oxygen by the electron transport chain of chloroplasts during assimilation of carbon dioxide. Biochim. Biophys. Acta **408**, 252-268.

Evans, M. C. W. and G. Bredenkamp (1990) The structure and function of the photosystem I reaction centre. Physiol. Plantarum. **79**, 415-420.

Förster, T. (1948) Intermolecular energy transfer and fluorescence. Ann. Phys. Leipzig **2**, 55-75.

Forti, G., A. Cappelletti, R. L. Nobili, F. M. Garlaschi, P. D. Gerola and R. C. Jennings (1983) Interactions of ferredoxin and ferredoxin-NADP reductase with thylakoids. Arch. Biochem. Biophys. **221**, 507-513.

Forti, G. and P. M. G. Grubas (1985) Two sites of interaction of ferredoxin with thylakoids. FEBS Lett. **186**, 149-152.

Foust, G. P., S. G. Mayhew and V. Massey (1969) Complex formation between ferredoxin triphosphopyridine nucleotide reductase and electron transfer proteins. J. Biol. Chem. **244**, 964-970.

Furbank, R. T., M. R. Badger and C. B. Osmond (1982) Photosynthetic oxygen exchange in isolated cells and chloroplasts of C_3 plants. Plant Physiol. **70**, 927-931.

Furbank, R. T. and M. R. Badger (1983) Oxygen exchange associated with electron transport and photophosphorylation in spinach thylakoids. Biochem. Biophys. Acta **723**, 400-409.

Garab, G. and G. Hind (1987) Cyclic electron transport around photosystem I in washed thylakoids. In: Progress in Photosynthesis Research (J. Biggins, ed.), Vol. 2, pp. 541-544. Martinus Nijhoff Publishers, Dordrecht.

Garab, G., Y. Hong, S. J. Coughlan, H. C. P. Matthijs and G. Hind (1990) Absorbance transients of ferredoxin:$NADP^+$ reductase in isolated thylakoid membranes. In: Current Research in Photosynthesis (M. Baltscheffsky, ed.), Vol. 2, pp. 667-670. Kluwer Academic Publishers, Dordrecht.

Gherichер, H. (1977) Photovoltaic phenomena in electochemical cells. In: Special topics in electrochemistry (P. Rock, ed.), Elsevier Scientific Pub. Co., Amsterdam. pp. 28-45.

Golbeck, J. H. (1987) Structure, function and organization of the photosystem I reaction center complex. Biochem. Biophys. Acta **895**, 167-204.

Good, N. and R. Hill (1955) Photochemical reduction of oxygen in chloroplasts. Arch. Biochem. Biophys. **57**, 355-366.

Goodwin, T. W. and G. Britton (1988) Distribution and Analysis of Carotenoids. In: Plant Pigments (T. W. Goodwin, ed.), Academic Press, London. pp. 61-132.

Gräber, P. (1987) Primary charge separation and energy transduction in photosynthesis. In: Bioelectrochemistry II (G. Milazzo and M. Blanks, eds.), Plenum Publishing, New York. pp. 379-429.

Greenbaum, E. (1985) Platinized chloroplasts: a novel photocatalytic material. Science **230**, 1373-1375.

Greenbaum, E. (1989) Biomolecular electronics: observations of oriented photocurrents by entrapped platinized chloroplasts. Bioelectrochem. Bioenerg. **21**, 171-177.

Greenbaum, E. (1990) Vectorial photocurrents and photoconductivity in metalized chloroplasts. J. Phys. Chem. **94**, 6151-6153.

Gregory, R. P. F. (1989) Photosynthesis. Blackie and Son Ltd., Glasgow. p. 93.

Gross, E. L., D. R. Youngman and S. L. Winemiller (1978) An FMN-photosystem I photovoltaic cell. Photochem. Photobiol. **28**, 249-256.

Guigliarelli, B., J. Guillaussier, P. Bertrand, J.-P. Gayda and P. Sétif (1989) Evidence for only one iron-sulfur cluster in center X of photosystem I from higher plants. J. Biol. Chem. **264**, 6025-6028.

Haehnel, W., R. (1984) Photosynthetic electron transport in higher plants. Ann. Rev. Plant Physiol. **35**, 659-693.

Haehnel, W., R. Ratajczak and H. Robenek (1989) Lateral distribution and diffusion of plastocyanin in chloroplast thylakoids. J. Cell Biol. **108**, 1397-1405.

Halliwell, B. (1981) Toxic effects of oxygen on plant tissues. In: Chloroplast metabolism, Oxford University Press, Oxford. pp. 179-205.

Hasumi, H., E. Nagata and S. Nakamura (1983) Molecular Heterogeneity of ferredoxin-$NADP^+$ reductase from spinach leaves. Biochem. Biophys. Res. Comm. **110**, 280-286.

Hauska, G. (1988) Phylloquinone in photosystem I: are quinones the secondary electron acceptors in all types of photosynthetic reaction centers? TIBS **13**, 415-416.

Heber, U., H. Egneus, U. Hanck, M. Jensen and S. Köster (1978) Regulation of photosynthetic electron transport

and photophosphorylation in intact chloroplasts and leaves of Spinacia oleracea L. Planta, **143**, 41-49.

Hill, R. and F. Bendall (1960) Function of the two cytochrome components in chloroplasts. A working hypothesis. Nature, **186**, 136-137.

Hippler, M., R. Ratajczak and W. Haehnel (1989) Identification of the plastocyanin binding subunit of photosystem I. FEBS Lett. **250**, 280-284.

Hirasawa, M., M. Boyer, K. Gray, D. Davis and D. B. Knaff (1987) The interaction of ferredoxin with chloroplast ferredoxin-linked enzymes. In: Progress in Photosynthesis Research (J. Biggins, ed.), Vol. 3, pp. 435-438. Martinus Nijhoff Publishers, Dordrecht.

Hirasawa, M., K.-T. Chang, K. J. Morrow Jr., and D. B. Knaff (1989) Circular dichroism, binding and immunological studies of the interaction between spinach ferredoxin and glutamate synthase. Biochim. Biophys. Acta **977**, 150-156.

Hoj, P. B., I. Svendson, H. V. Scheller and B. L. Moller (1987) Identification of a chloroplast-encoded 9-kDa polypeptide as a 2[4Fe-4S] protein carrying centers A and B of photosystem I. J. Biol. Chem. **262**, 12676-12684.

Hosein, B. and G. Palmer (1983) The kinetics and mechanism of oxidation of reduced spinach ferredoxin by molecular oxygen and its reduced products. Biochim. Biophys. Acta **723**, 383-390.

Hossain, M. A., Y. Nakano and K. Asada (1984) Monodehydroascorbate reductase in spinach chloroplasts and its participation in regeneration of ascorbate for scavenging hydrogen peroxide. Plant Cell Physiol. **25**, 385-395.

Hurt, E. C. and G. Hauska (1982) Oxidant-induced reduction of cytochrome b_6 in the isolated cytochrome b_6/f complex from chloroplasts. Photobiochem. Photobiophys. **4**, 9-15.

Itoh, S., M. Iwaki, I. Ikegami (1987) Extraction of vitamin K-1 from photosystem I particles by treatment with diethyl ether and its effects on the A_1^- EPR signal and system I photochemistry. Biochim. Biophys. Acta **893**, 508-516.

Izawa, S. and R. L. Pan (1978) Photosystem I electron transport and phosphorylation supported by electron

donation to the plastoquinone region. Biochem. Biophys. Res. Comm. **83**, 1171-1177.

Izawa, S. (1980) Acceptors and donors for chloroplast electron transport. Meth. Enzymol. **69**, 413-434.

Jablonski, P. P. and J. W. Anderson (1981) Light-dependent reduction of dehydroascorbate by reptured pea chloroplasts. Plant Physiol. **67**, 1239-1244.

Jablonski, P. P. and J. W. Anderson (1982) Light-dependent reduction of hydrogen peroxide by reptured pea chloroplasts. Plant Physiol. **69**, 1407-1413.

Jennings, R. C. and Forti, G. (1974) Involvement of oxygen during photosynthetic inductions. In: Proceedings of the third international congress on photosynthesis (M. Avron, ed.), Elsevier, Amsterdam. pp. 735-743.

Joliot, P. and A. Joliot (1986) Mechanisms of proton-pumping in the cytochrome b/f complex. Photosynth. Res. **9**, 113-124.

Karplus, P. A., K. A. Walsh and J. R. Herriott (1984) Amino acid sequence of spinach ferredoxin:$NADP^+$ oxioreductase. Biochemistry **23**, 6576-6583.

Kim, D., K. Yoshihara and I. Ikegami (1989) Picosecond photochemistry of P700-enriched and vitamin K_1-depleted photosystem I particles isolated from spinach. Plant Cell Physiol. **30**, 679-684.

Koryta, J., J. Dvorak and V. Bohachova (1970) Electrochemistry. Methuen and Co., London. pp. 311-313.

Kyle, D. (1985) The 32 000 Dalton Q_B protein of photosystem II. Photochem. Photobiol. **41**, 107-116.

Lagoutte, B. and P. Mathis (1989) The photosystem I reaction centre: structure and photochemistry. Photochem. Photobiol. **49**, 833-844.

Lemieux, S. and R. Carpentier (1988a) Properties of immobilized thylakoid membranes in a photosynthetic photoelectrochemical cell. Photochem. Photobiol. **48**, 115-121.

Lemieux, S. and R. Carpentier (1988b) Properties of a photosystem II preparation in a photoelectrochemical cell. J. Photochem. Photobiol. B: Biol. **2**, 221-231.

Lehniger, A. L. (1982) Principles of Biochemistry. Worth Publishers, Inc., New York. p. 655.

Malmström, B. G. (1989) The mechanism of proton translocation in respiration and photosynthesis. FEBS Lett. **250**, 9-21.

Marscho, T. V., P. W. Behrens and R. J. Radmer (1979) Photosynthetic oxygen reduction in isolated intact chloroplasts and cells from spinach. Plant Physiol. **64**, 656-659.

Matthijs, H. C. P., S. J. Coughlan and G. Hind (1987) Ferredoxin-$NADP^+$ oxioreductase: studies on the thylakoid membrane bound enzyme. In: Progress in Photosynthesis Research (J. Biggins, ed.), Vol. 2, pp. 545-548. Martinus Nijhoff Publishers, Dordrecht.

McPherson, P. H., M. Y. Okamura and G. Feher (1990) Electron transfer from the reaction center of Rb. sphaeroides to the quinone pool: doubly reduced Q_B leaves the reaction center. Biochim. Biophys. Acta **1016**, 289-292.

Mehler, A. (1951) Studies on reactions of illuminated chloroplasts. I. Mechanism of the reduction of oxygen and other Hill reagents. Arch. Biochem. Biophys. **33**, 65-77.

Melis, A. (1989) Spectroscopic methods in photosynthesis: photosystem stoichiometry and chlorophyll antenna size. Phil. Trans. R. Soc. Lond. B **323**, 397-409.

Mills, J. D., R. E Slovacek and G. Hind (1978) Cyclic electron transport in isolated intact chloroplasts. Biochim. Biophys. Acta **504**, 298-309.

Mimeault, M. and R. Carpentier (1989) Kinetics of photocurrent induction by a thylakoid containing electrochemical cell. Bioelectrochem. Bioenerg. **22**, 145-158.

Mimuro, M. (1990) Studies on excitation energy flow in the photosynthetic pigment system; structure and energy transfer mechanism. Bot. Mag. Tokyo **103**, 233-253.

Mitchell, P. (1961) Coupling of phosphorylation to electron and hydrogen transfer by a chemi-osmotic type of mechanism. Nature **191**, 144-148.

Mitchell, P. (1975) The protonmotive Q cycle: a general formulation. FEBS Lett. **59**, 137-139.

Nakano, Y. and K. Asada (1980) Spinach chloroplast scavenge hydrogen peroxide on illumination. Plant Cell Physiol. **21**, 1295-1307.

Nakano, Y. and K. Asada (1981) Hydrogen peroxide is scavenged by ascorbate-specific peroxidase in spinach chloroplasts. Plant Cell Physiol. **22**, 867-880.

Nanba, M. and S. Katoh (1986) The site and mechanism of duroquinol oxidation by cytochrome b_6-f complex in Synechococcus sp. Biochim. Biophys. Acta **851**, 484-490.

Nugent, J. H. A., A. Telfer, C. Demetriou and J. Barber (1989) Electron transfer in the isolated photosystem II reaction center complex. FEBS Lett. **255**, 53-58.

Pagani, S., G. Vecchio, S. Iametti, R. Bianchi and F. Bonomi (1986) On the role of the 2Fe-2S cluster in the formation of the structure of spinach ferredoxin. Biochim. Biophys. Acta **870**, 538-544.

Pan, R. L., I-Ji Fan, R. Bhardwaj and E. L. Gross (1982) A photosynthetic photoelectrochemical cell using flavin mononucleotide as the electron acceptor. Photochem. Photobiol. **35**, 655-664.

Peters, F. A. L. J., J. E. van Wielink, H. W. Wong Fong Sang, S. de Vries and R. Kraayenhof (1983) Studies on well coupled photosystem I-enriched subchloroplast vesicles. Content and redox properties of electron-transfer components. Biochim. Biophys. Acta **722**, 460-470.

Pfister, K. and C. J. Arntzen (1979) Mode of action of photosystem II-specific inhibitors in herbicide resistant weed biotypes. Z. Naturforsch. C. **34**, 996-1009.

Pschorn, R., W. Ruehle and A. Wild (1987) The influence of the proton gradient on the activation of ferredoxin-$NADP^+$-oxioreductase by light. Z. Naturforsch. **43c**, 207-212.

Reilly, P. and N. Nelson (1988) Photosystem I complex. Photosynth. Res. **19**, 73-84.

Rich, P. and D. S. Bendall (1980) The redox potential fo the b-type cytochrome of higher plant chloroplasts. Biochim. Biophys. Acta **591**, 153-161.

Robinson, J. M. (1988) Does O_2 photoreduction occur within chloroplasts in vivo? Physiol. Plantarum **72**, 666-680.

Rüdiger, W. and S. Schoch (1988) Chlorophylls. In: Plant Pigments (T. W. Goodwin, ed.), Academic Press, London. pp. 1-59.

Rutherford, A. W. (1988) Photosystem II, the oxygen evolving photosystem. In: Light-energy transduction in photosynthesis: Higher Plant and Bacterial Models (S. E. Stevens and D. A. Bryant, eds.), Am. Soc. Plant Physiol., New York. pp. 163-177.

Salin, M. (1987) Toxic oxygen species and protective mechanisms of the chloroplast. Physiol. Plantarum **72**, 681-689.

Sanderson, D. G., E. L. Gross and M. Seibert (1987) A photosynthetic photoelectrochemical cell using phenazine methosulfate and phenazine ethosulfate as electron acceptors. App. Biochem. Biotech. **14**, 1-20.

Sawyer, D. T. and J. S. Valentine (1981) How super is superoxide? Acc. Chem. Res. **14**, 393-400.

Schatz, G. H., H. Brock and A. R. Holzwarth (1988) Kinetic and energetic model for the primary processes in photosystem II. Biophys. J. **54**, 397-405.

Scheller, H. V., P. B. Hoj, I. Svendson and B. L. Moller (1988) Partial amino acid sequences of two nuclear-encoded photosystem I polypeptides from barley. Biochim. Biophys. Acta **933**, 501-505.

Scheller, H. V., I. Svendson and B. L. Moller (1989) Subunit composition of photosystem I and identification of center X as a [4Fe-4S] iron-sulfur cluster. J. Biol. Chem. **264**, 6929-6934.

Scheller, H. V. and B. L. Moller (1990) Photosystem I polypeptides. Physiol. Plantarum **78**, 484-494.

Sétif, P. and H. Bottin (1989) Identification of electron-transfer reactions involving the acceptor A_1 of photosystem I at room temperature. Biochemistry **28**, 2689-2697.

Sheriff, S. and J. R. Herriott (1981) Structure of ferredoxin-$NADP^+$ oxioreductase and the location of the NADP binding site. J. Mol. Biol. **145**, 441-451.

Shuvalov, V. A., A. M. Nuijs, H. J. van Gorkom, H. W. J. Smit and L. N. M. Duysens (1986) Picosecond absorbance changes upon selective excitation of the primary electron donor P700 in photosystem I. Biochem. Biophys. Acta **850**, 319-323.

Singer, S. G. and G. L. Nicolson (1972) The fluid mosaic model of the structure of cell membranes. Cell membranes are viewed as two dimensional solutions of

oriented globular proteins and lipids. Science **175**, 720-731.

Steiger, H.-M. and E. Beck (1981) Formation of hydrogen peroxide and oxygen dependence of photosynthetic CO_2 assimilation by intact chloroplasts. Plant Cell. Physiol. **22**, 561-576.

Tagawa, K., H. Y. Tsujimoto and D. I. Arnon (1963) Proc. Natl. Acad. Sci. USA **49**, 567-572.

Takahashi, M. and K. Asada (1988) Superoxide production in the aprotic interior of chloroplast thylakoids. Arch. Biochem. Biophys. **267**, 714-722.

Tarashevich, M. R. and K. A. Radyushkina (1970) Determination of kinetic parameters of electrochemical reactions of oxygen and hydrogen peroxide. Soviet Electrochem. **6**, 786-795.

Trissl, H.-W. and W. Leibl (1989) Primary charge separation in photosystem II involves two electrogenic steps. FEBS Lett. **244**, 85-88.

Volkov, A. G. (1989) Oxygen evolution in the course of photosynthesis: molecular mechanisms. Bioelectrochem. Bioenerg. **21**, 3-24.

Wasielewski, M. R., D. G. Johnson, M. Seibert and Govindjee (1989) Determination of the primary charge separation rate in isolated photosystem II reaction centers with 500-fs time resolution. Proc. Natl. Acad. Sci. USA **86**, 524-528.

Wikstrom, M., K. Krab and M. Sanaste (1981) Proton translocating cytochrome complexes. Ann. Rev. Biochem. **50**, 623-655.

Wolosuik, R. A. and B. B. Buchanan (1977) Thioredoxin and glutathione regulate photosynthesis in chloroplasts. Nature **266**, 565-567.

Wood, P. M. and D. S. Bendall (1975) The kinetics and specificity of electron transfer from cytochromes and copper proteins to P700. Biochim. Biophys. Acta **387**, 115-128.

Wynn, R. and R. Malkin (1988) Characterization of an isolated chloroplast membrane FeS protein and its identification as the photosystem I $Fe\text{-}S_A/Fe\text{-}S_B$ binding protein. FEBS Lett. **229**, 293-298.

Yocum, C. F., N. Nelson and E. Racker (1975) A combined procedure for preparation of plastocyanin, ferredoxin and CF_1. Preparative Biochem. **5**, 305-317.

Zanetti, G. and B. Curti (1980) Ferredoxin-$NADP^+$ oxioreductase. Methods Enzymol. **69**, 250-255.

Zanetti, G. and B. Curti (1981) Interactions between ferredoxin-$NADP^+$ reductase and ferredoxin at different reduction levels of the two proteins. FEBS Lett. **129**, 201-204.

Opening quotes taken from:

Polanyi, Michael (1969) The logic of tacit interference. In: Knowing and Being: Essays by Michael Polanyi (M. Grene, ed.), University of Chicago Press, Chicago. p. 151.

Siberry, Jane (1989) Bound by the beauty. From the LP: Bound by the beauty (J. Siberry and J. Switzer, producers), Duke Street Records, Toronto. (Words and music, copyright 1989, wing-it/red sky music).